

# Myxothiazol induced reverse reaction in *Rhodobacter capsulatus* cytochrome bc1 mutants

---

Kralj, Tomica

Master's thesis / Diplomski rad

2015

*Degree Grantor / Ustanova koja je dodijelila akademski / stručni stupanj:* **University of Split, University of Split, Faculty of science / Sveučilište u Splitu, Prirodoslovno-matematički fakultet**

*Permanent link / Trajna poveznica:* <https://urn.nsk.hr/urn:nbn:hr:166:844393>

*Rights / Prava:* [Attribution-NonCommercial-ShareAlike 4.0 International](#)/[Imenovanje-Nekomercijalno-Dijeli pod istim uvjetima 4.0 međunarodna](#)

*Download date / Datum preuzimanja:* **2024-11-26**

*Repository / Repozitorij:*

[Repository of Faculty of Science](#)



University of Split  
Faculty of Science  
Department of Physics

**Myxothiazol induced reverse reaction in *Rhodobacter  
capsulatus* cytochrome bc<sub>1</sub> mutants**

Tomica Kralj

Graduation thesis

Split, 2015.

## Summary

Cytochrome  $bc_1$  (also known as complex III) is an enzyme of electron transport chain and is found in both bacteria and mitochondria. It has an important role in cellular respiration as it contributes to the generation of the proton motive force which is later used for ATP synthesis. It does this by coupling oxidation and reduction of quinones (commonly called Q-cycle) to proton translocation across inner mitochondrial or bacterial plasma membrane. Stable semiquinone is formed in one of the catalytic sites of cytochrome  $bc_1$  ( $Q_i$  site) during its enzymatic activity. We analysed mutants of cytochrome  $bc_1$  that were thought to have even more stable semiquinone than wild type due to steric hinderance introduced at the  $Q_i$  site. Experiments performed on *Rhodobacter capsulatus* mutants indicate that during reverse reaction hemes  $b_H$  get reduced more than in the same reaction in wild type. However, despite this no semiquinone signal could be detected at  $Q_i$  site in those mutants.

**Supervisor:** doc. dr. sc. Marija Raguž

**Co-supervisor:** prof. dr. sc. hab. Artur Osyczka

**Reviewers:** prof. dr. sc. Ante Bilušić, doc. dr. sc. Stjepan Orhanović

This research was done as ERASMUS internship in Molecular Bioenergetics Group of Jagiellonian University in Krakow, Poland. I would like to take this opportunity to thank everyone from the group for making me feel welcome and helping me with practical work and theoretical understanding of the subject.

I would specially like to thank prof. dr. Artur Osyczka for accepting me as a guest student and for his valuable guidance and advice throughout the course of the research, and dr. Rafał Pietras for his tutoring and generous help with this thesis.

Sveučilište u Splitu  
Prirodoslovno-Matematički Fakultet  
Odjel za Fiziku

**Povratna reakcija u *Rhodobacter capsulatus* citokrom bc<sub>1</sub>  
mutantima inducirana inhibitorom miksotiazolom**

Tomica Kralj

Diplomski rad

Split, 2015.

## Sažetak

Citokrom  $bc_1$  (također poznat i kao kompleks III) je enzim transportnog lanca elektrona te ga se može naći u bakterijama i mitohondrijima. Ima važnu ulogu u staničnom disanju, budući da doprinosi stvaranju elektrokemijskog gradijenta protona koji se kasnije koristi za sintezu ATP-a. To čini tako da spaja oksidaciju i redukciju kinona (zajednički nazvane Q ciklus) sa premještanjem protona preko unutarnje membrane mitohondrija ili plazma membrane bakterija. Tijekom ove enzimatske aktivnosti, stabilni semikinon se stvara u jednom od katalitičkih mjesta citokroma  $bc_1$  ( $Q_i$  mjesto). Analizirali smo mutante citokroma  $bc_1$  za koje se smatralo da bi mogli imati još stabilniji semikinon nego divlji tip zbog prostornih smetnji induciranih u  $Q_i$  mjestu. Pokusi rađeni na *Rhodobacter capsulatus* mutantima ukazuju da su tijekom povratne reakcije hemovi  $b_H$  reducirani više nego tijekom iste reakcije u divljem tipu. Ipak, unatoč tome nije bilo moguće opaziti nikakav signal semikinona u  $Q_i$  mjestu u tim mutantima.

**Mentor:** doc. dr. sc. Marija Raguž

**Komentor:** prof. dr. sc. hab. Artur Osyczka

**Recenzenti:** prof. dr. sc. Ante Bilušić, doc. dr. sc. Stjepan Orhanović

## Table of Contents

1. Introduction.....	7
1.1. Oxidative phosphorylation.....	7
1.2. Structure and mechanism of action of cytochrome bc1.....	8
1.3. Research goal.....	10
2. Materials and methods.....	11
2.1. Materials.....	11
2.2. Bacterial cultivation and isolation of proteins.....	12
2.2.1. Choice of mutants.....	12
2.2.2. Procedure for growing bacteria.....	14
2.2.3. Isolation of proteins and preparation of chromatophores.....	14
2.3. Optical spectroscopy.....	16
2.3.1 Theory.....	16
2.3.2. Concentration measurements.....	17
2.3.3. Protein activity measurements.....	18
2.3.4. Reactive oxygen species (ROS) production measurements.....	18
2.4. Flash activated electron transfer in chromatophores.....	19
2.4.1. Theory.....	19
2.4.2. Experimental procedure.....	20
2.5. Electron paramagnetic resonance spectroscopy.....	21
2.5.1. Theory.....	21
2.5.2. Experimental procedure.....	25
3. Results and discussion.....	27
3.1 Optical spectroscopy measurements.....	27
3.2. Flash spectroscopy measurements.....	28
3.3. EPR measurements of semiquinone.....	32
3.4. Power saturation.....	33
3.5. Potentiometric titration of semiquinone.....	36
3.6. EPR measurements of hemes b.....	37
3.7. ROS production measurements.....	39
4. Conclusions.....	40
5. References.....	42

# 1. Introduction

## 1.1. Oxidative phosphorylation

All forms of life use adenosine triphosphate (ATP) to power biochemical reactions. To synthesize ATP most heterotrophic organisms primarily use oxidative phosphorylation – series of metabolic pathways which in eukaryotes take place in the inner membrane of mitochondria and in bacteria in their plasma membrane. Protein complexes and their cofactors that participate in oxidative phosphorylation are commonly called electron transport chain. There, chemical energy from nutrients is converted to proton gradient - a difference in proton concentration on two sides of the membrane, and charge gradient - difference in electrical potential across the membrane, also caused by charged protons.

This proton concentration and charge gradients together form electrochemical gradient - proton motive force. Proton motive force drives the ATP synthase which binds adenosine diphosphate and inorganic phosphate to form ATP. The proton gradient is established through the working of protein complexes which translocate protons – in mitochondria those are complexes I, III and IV of the electron transport chain (fig. 1).

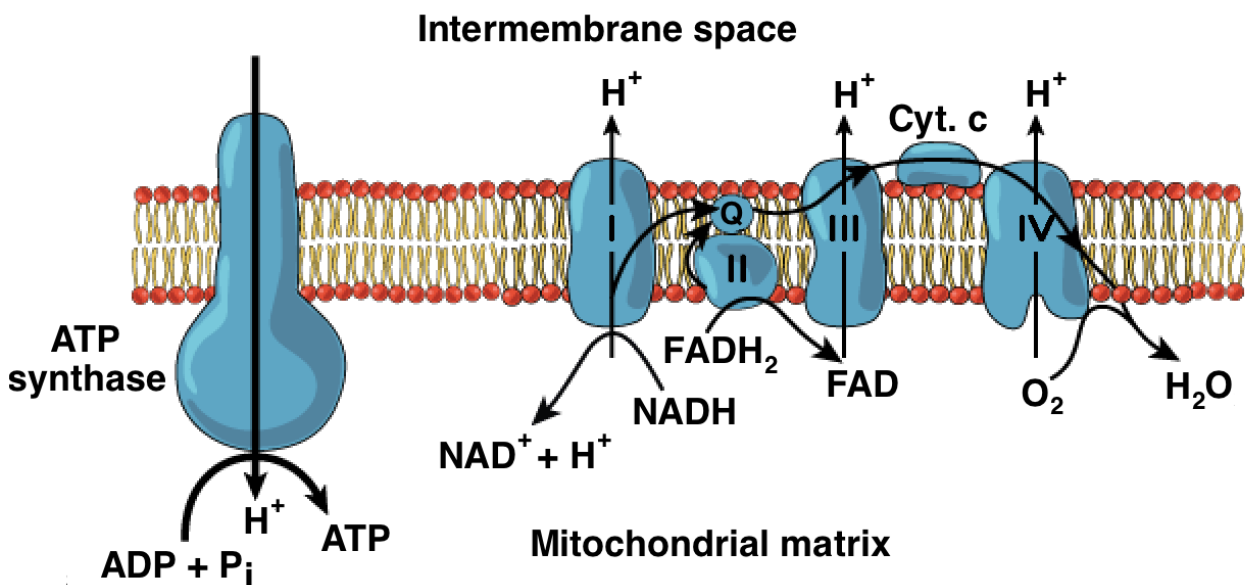


Figure 1: electron transport chain in the inner membrane of mitochondria, with complexes I, II, III and IV and ATP synthase.



## 1.2. Structure and mechanism of action of cytochrome bc<sub>1</sub>

In this research we focused on cytochrome bc<sub>1</sub>, also known as complex III of the electron transport chain. This protein has a crucial part in generating ATP in most eukaryotes and procaryotes, its main function being oxidation and reduction of quinones and reduction of cytochrome c [1].

In the cellular environment, there are two substrates of cytochrome bc<sub>1</sub> – quinone and cytochrome c. Cytochrome c is a hemoprotein and serves as an electron carrier. It is highly soluble in water and moves through intermembrane space of mitochondria or periplasmic space in bacteria, transferring electrons between cytochrome bc<sub>1</sub> and complex IV of electron transport chain.

Quinones are a class of aromatic organic compounds which serve as both electron and proton carriers. Any quinone can carry two electrons and two protons, coming in several oxidation states: fully oxidised form – ubiquinone (Q), partially reduced form – semiquinone (SQ), and fully reduced form – quinol (QH<sub>2</sub>) (fig. 2). They are hydrophobic and thus move within mitochondrial inner membrane, transferring electrons from complexes I and II to complex III of the electron transport chain. The stock of quinones present in the membrane, regardless of the oxidation state, is referred to as quinone pool. Complexes I and II put electrons in quinone pool by reducing Q to QH<sub>2</sub>. Cytochrome bc<sub>1</sub> accepts electrons from the pool by oxidizing QH<sub>2</sub> back to Q and transfers the electrons to complex IV by reducing cytochrome c (which is later oxidized by complex IV).

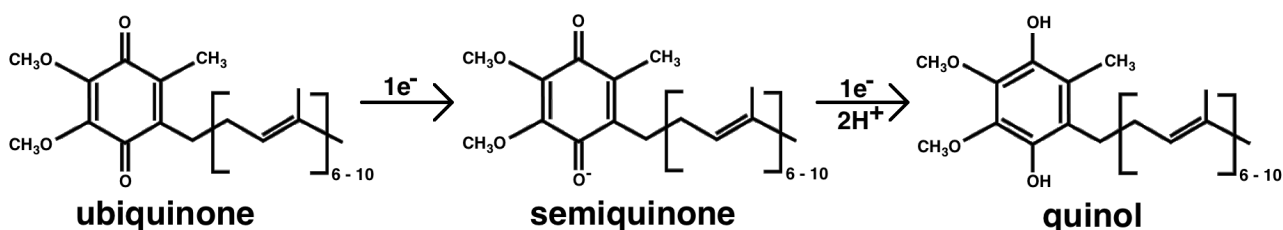


Figure 2: structure of ubiquinone (left), semiquinone (centre) and quinol (right): aromatic head and hydrophobic aliphatic tail of 6-10 isoprenyl subunits.

Cytochrome bc<sub>1</sub> is a homodimer, with each monomer having four redox cofactors: hemes b<sub>L</sub> and b<sub>H</sub>, which together form low-potential chain, and iron-sulphur cluster and heme c<sub>1</sub> which together form high-potential chain [2] (fig. 3). In b<sub>L</sub> and b<sub>H</sub>, L stands for low and H for high potential, relative to one another. In description of the protein and later description of the experiments we performed, focus will always be on just one part of the dimer (one monomer).

There are two active sites for quinone - Qi and Qo site. “i” and “o” mark whether protons are taken in or released out of the site. In standard conditions, QH<sub>2</sub> binds to Qo site and Q binds to Qi site. At the Qo site, one electron from QH<sub>2</sub> goes to heme b<sub>L</sub>, from there to heme b<sub>H</sub>, and from there to SQ or Q which are at the Qi site. The other electron from QH<sub>2</sub> goes to iron-sulphur cluster, from there to heme c<sub>1</sub> and from there to cytochrome c. It is not yet known whether this oxidation reactions are consecutive or simultaneous. Iron-sulphur cluster is not fixed, but attached to the rest of the complex only on one side of a long hinge and can thus move between Qo site and heme c<sub>1</sub> [3]. This means that when iron-sulphur cluster is in position to transfer electrons to heme c<sub>1</sub>, it cannot immediately take electrons from heme b<sub>L</sub>. This mechanism prevents electrons leaking from low to high-potential chain and minimizes the danger of short circuit.

During the oxidation reactions two protons from QH<sub>2</sub> at Qo site are released into inter-membrane space. In Qi site, as Q is reduced it also binds two protons from mitochondrial matrix. Since only one electron goes from Qo to Qi site, firstly Q is reduced to SQ and then, as another QH<sub>2</sub> molecule comes to Qo site, SQ is fully reduced to QH<sub>2</sub>. This means it takes two QH<sub>2</sub> molecules at the Qo site to fully reduce one Q molecule at the Qi site. This oxidation and reduction of quinones in cytochrome bc<sub>1</sub> is called Q-cycle. The net result of this reactions is intake of 2 protons from the matrix and releasing of 4 protons into inter-membrane space per cycle - this is how cytochrome bc<sub>1</sub> translocates protons.

This mode of operation is called forward reaction. However, cytochrome bc<sub>1</sub> turnover is completely reversible – both the Q cycle and high potential chain reactions [4]. In reverse reaction QH<sub>2</sub> binds not to Qo but to Qi site and reduces heme b<sub>H</sub>, leaving SQ at the Qi site. Only heme b<sub>H</sub> gets reduced because the redox potential of heme b<sub>L</sub> is lower than that of b<sub>H</sub> and therefore electrons don't go in that direction. This reverse reaction can be readily observed when Qo site activity is terminated by binding of inhibitors such as myxothiazol or stigmatellin.

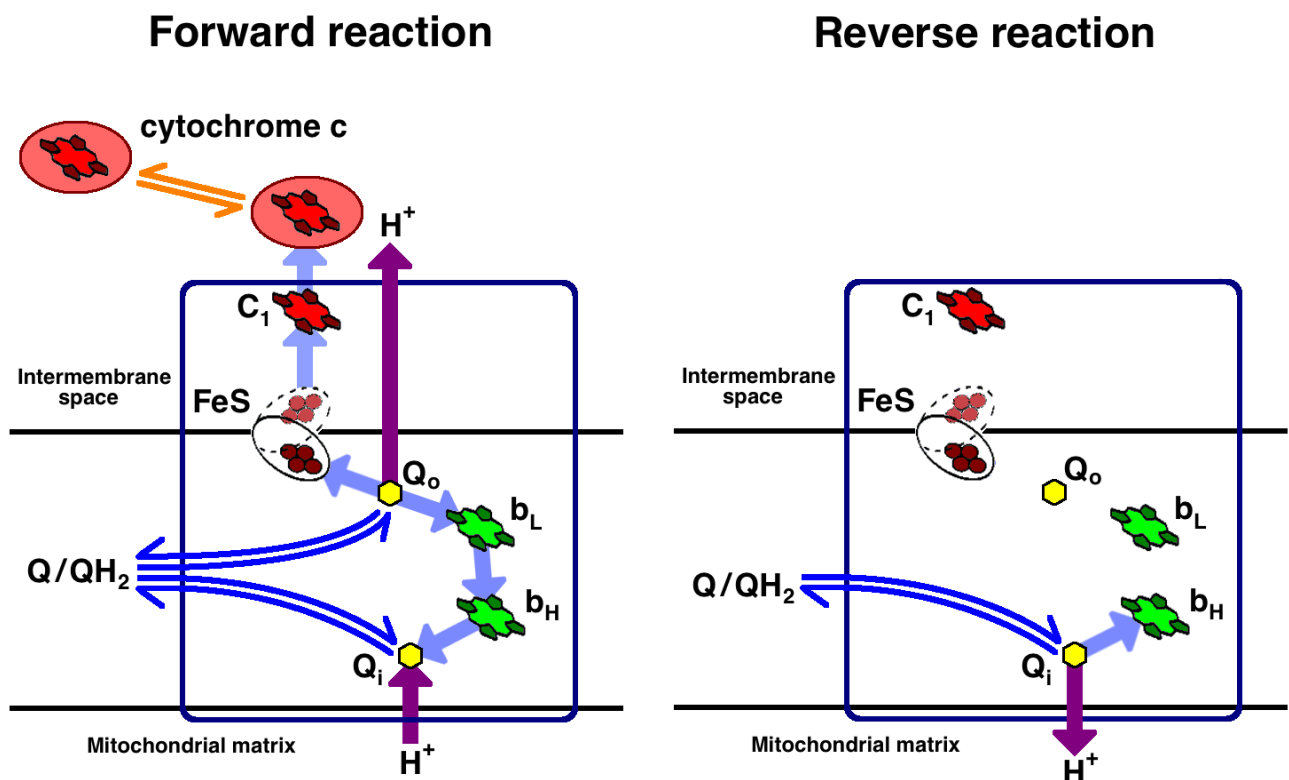


Figure 3: scheme and modes of operation of cytochrome  $bc_1$ , with high (red) and low (green) potential chains,  $Q_i$  and  $Q_o$  sites (yellow) and attached cytochrome  $c$  (pink). Flow of electrons is depicted in light blue, and flow of protons in purple.

### 1.3. Research goal

The main idea of this research was to gain additional knowledge about stability of SQ in the  $Q_i$  site of cytochrome  $bc_1$  and to incorporate that into the existing knowledge about structure and mechanism of catalysis of  $Q_i$  site. We wanted to investigate whether it is possible to increase the lifetime of SQ in the site, which was to be done by hindering the movement of SQ in and out of the site using two *R. capsulatus* mutants.

## 2. Materials and methods

### 2.1. Materials

Chemicals and solutions used for bacterial growth and isolation of proteins:

- MPYE medium
  - bacto peptone
  - yeast extract
  - $MgCl_2$
  - $CaCl_2$
- MOPS - 3-morpholinopropane-1-sulfonic acid
- Tris – 2-Amino-2-hydroxymethyl-propane-1,3-diol
- kanamycin
- proteolysis inhibitors:
  - BH - benzydamine hydrochloride
  - 6-ACA - 6-aminocaproic acid
  - PMFS - phenylmethylsulfonyl fluoride

Chemicals used in the experiments:

- myxothiazol
- antimycin
- $DBH_2$  – 2,3-dimethoxy-5-decyl-6-methyl-1,4-benzoquinol
- potassium ferricyanide –  $K_3[Fe(CN)_6]$
- ascorbate (L-ascorbic acid, vitamin C)
- sodium dithionite –  $Na_2S_2O_2$
- valinomycin
- Mediators used in flash experiments and potentiometric titration of chromatophores:
  - QH – quinhydrone
  - DAD – 2,3,5,6-tetramethyl-1,4-phenylenedimine
  - NQS – 1,2-naphtoquinone-4-sulphonate
  - NQ – 1,2-naphtoquinone

- PMS – phenazine methosulphate
- PES – phenazine ethosulphate
- DQ – duroquinone
- ITS – indigo-trisulfonate
- HNQ – 2-hydroxy-1,4-naphthoquinone
- AQS – anthraquinone-2-sulphoric acid

## 2.2. Bacterial cultivation and isolation of proteins

### 2.2.1. Choice of mutants

All of the experiments were performed using bacterial cytochrome  $bc_1$  from *Rhodobacter capsulatus*. While mitochondrial cytochrome  $bc_1$  is a large complex that contains up to 11 subunits, depending on the species, bacterial contains only three or four (fig. 4) [5]. However, those subunits are highly homologous to their mitochondrial counterparts and thus the complex is functionally very similar, making this system suitable for studying cytochrome  $bc_1$  in general [6].

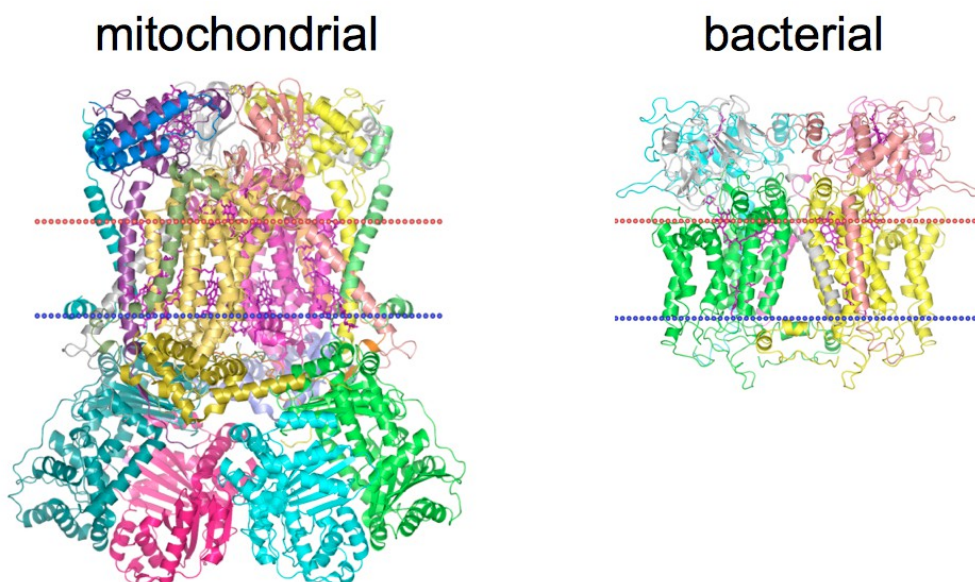


Figure 4: mitochondrial (left) and bacterial (right) cytochrome  $bc_1$

*R. capsulatus* has photosynthetic chains that consist of just two membranous complexes, photosynthetic reaction centre and cytochrome  $bc_1$ . Presence of photosynthetic reaction centre presents one of the advantages of using *R. capsulatus*. When excited by light, this reaction centre reduces Q and oxidises cytochrome c and it is thus coupled to cytochrome  $bc_1$ , making it possible to study kinetics of the reactions in cytochrome  $bc_1$  (in chromatophores, not isolated protein) by using flash activated optical spectroscopy [7].

There are several other experimental advantages of using cytochrome from *R. capsulatus*:

- it is easier to grow bacterial cells and obtain protein from them than from eukaryotic organisms
- the genetic manipulation is less complicated to perform in prokaryotic than in eukaryotic cells
- because bacteria can grow photosynthetically (autotrophically) only when cytochrome  $bc_1$  is functional, unviable mutations of the complex can easily be detected by observing the growth under photosynthetic conditions
- *R. capsulatus* can also be grown non-photosynthetically (heterotrophically), meaning that non-functional complexes of cytochrome  $bc_1$  can be obtained as well.

In this experiments we used two Qi site mutants of *R. capsulatus* – first containing two mutations where two isoleucines are replaced with tryptophan and phenylalanine (I47W and I213F) and second containing single mutation where just one isoleucine is replaced with tryptophan (I47W). These particular mutants were chosen because previous experiments showed much higher levels of reverse reaction in Qi site than in wild type, which meant there are possibly higher levels of SQ in Qi site. It was speculated those mutants may exhibit a steric hindrance in the entrance to Qi site due to tryptophan and phenylalanine being larger molecules than isoleucine (fig. 5). As a consequence, SQ would stay in the site for longer time, accumulating in higher levels which would be reflected in its stronger EPR signal. The mutants were acquired the strains from the stock already available at the laboratory and apart from them, we also used wild type as a control for all experiments..

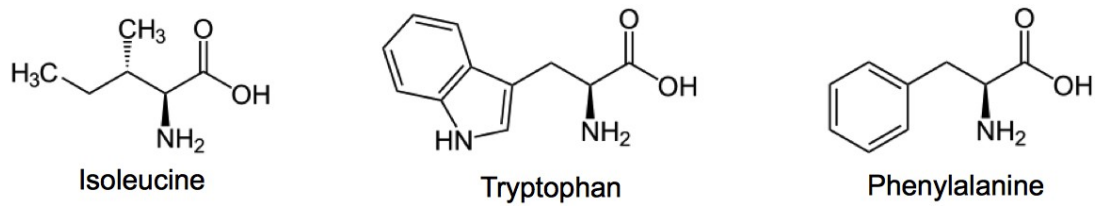


Figure 5: isoleucine, tryptophan and phenylalanine

### 2.2.2. Procedure for growing bacteria

Bacteria were taken from stock frozen in  $-80^{\circ}\text{C}$  and planted on MPYE gel plate. MPYE medium is made by adding 3g of bacto peptone, 3g of yeast extract, 1.6ml of 1M  $\text{MgCl}_2$  and 1ml of 1M  $\text{CaCl}_2$  to one liter of distilled water. After incubating for two days, bacteria were transferred first to 4-6 small flasks (containing 25ml of liquid MPYE per flask) where they incubated for 1 day, and then to 8-12 bigger flasks (1.25l of MPYE per flask) where they incubated for 3 days. Bacteria were always incubated at  $30^{\circ}\text{C}$  and in the dark, because they grow faster when feeding heterotrophically. Before use, all of the flasks were sterilized, together with medium, at  $110^{\circ}\text{C}$  for 15 min and sterile antibiotic kanamycin was added upon cooling. Both mutants and wild type used in this experiments were genetically engineered to be resistant to kanamycin, which is used to prevent contamination by other bacteria and to force *R. Capsulatus* to over express cytochrome  $bc_1$ . *R. Capsulatus* can survive without cytochrome  $bc_1$  in aerobic conditions because they have alternative quinol oxidases that use oxygen. Since genes for cytochrome  $bc_1$  and those for antibiotic resistance are in the same plasmid and since plasmid is always expressed as a whole, bacteria have to express resistance gene in order to survive which forces them to also express cytochrome  $bc_1$  genes.

### 2.2.3. Isolation of proteins and preparation of chromatophores

After the bacteria have fully grown they were concentrated by repeated centrifugation (6000 rpm for 30 min at  $4^{\circ}\text{C}$ ) in MOPS buffer (pH 7). Once concentrated to volume of approximately 200 ml (up to 400 ml for larger initial batches) they were pressed in French pressure cell press. This shatters plasma membrane and creates chromatophores - vesicles formed from membrane fragments that contain bacterial membrane proteins. Just before French-pressing, inhibitors 6-ACA, BH and

PMSF (full names in materials), which inhibit various cellular proteolytic enzymes, were added to prevent proteolysis of cytochrome  $bc_1$ . After French-pressing, chromatophores were centrifuged (14 000 rpm for 30 min at 4°C) and ultracentrifuged (45 000 rpm for 90 min at 4°C) to separate them from cellular debris. From here the procedure was different for preparation of chromatophores and for isolated proteins.

When obtaining chromatophores, there was one more cycle of ultracentrifugation (45 000 rpm for 70 min at 4°C) after which chromatophores were stored in Tris buffer with pH 8, at 4°C (they can be stored in those conditions for up to two weeks). The process of French-pressing inverts the membranes [8], meaning that the side of the protein normally exposed to inter-membrane space is now on the inside of the vesicle, and matrix side is now exposed to buffer. Chromatophores obtained in this way retain all membrane proteins and cofactors, and also most of the molecules present in the inter-membrane space, including cytochrome  $c$ .

When obtaining isolated proteins, 0.8 – 1.2 g of DDM dissolved in TRIS (0.1 g per one big flask of bacteria) was added to the solution of chromatophores to break the vesicles. DDM is an amphiphilic detergent and as such also has a role of enabling membrane proteins, which are hydrophobic, to solubilise in water. After this, ultracentrifugation (45 000 rpm for 70 min at 4°C) was used to separate solubilised membranes from the non-solubilised debris. Solution containing just bacterial membrane proteins was put on an chromatography column in order to separate cytochrome  $bc_1$  from the rest of the proteins. At first we tried using ion-exchange (BioGel) column but cytochrome  $bc_1$  denatured on it, which was suspected due to unusual colour of the final protein solution and confirmed by optical spectroscopy and SDS-PAGE (sodium dodecyl sulphate polyacrylamide gel electrophoresis) (fig. 6). We then tried using strep-tag column, a more delicate technique [9]. This proved to be successful, as again confirmed by optical spectroscopy and SDS-PAGE – in figure 6, on the right we can see the 3 characteristic lines of cytochrome  $bc_1$  (cytochrome  $b$ , cytochrome  $c_1$  and iron-sulphur cluster).



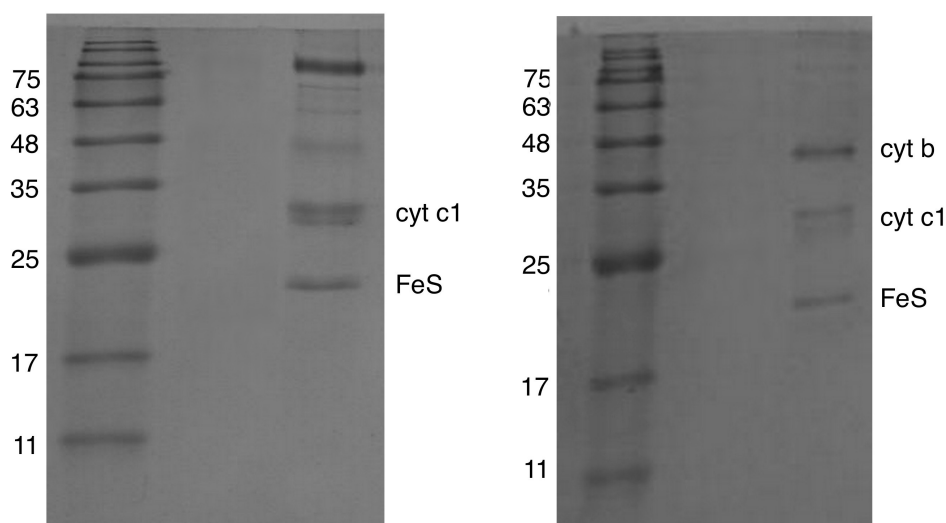


Figure 6: SDS-PAGE of double mutant protein after isolation with ion-exchange column (left) and strep-tag column (right). The column on the left in both pictures is a reference ladder, the numbers on the right are kilodaltons (kDa).

From then on, we isolated proteins exclusively using strep-tag column. We used both mutants and wild type with strep-tag sequence on cytochrome  $bc_1$  (all of which were also available in stock). Even though wild type can be isolated on ion-exchange column as well, we used strep-tag column in order to have all of the samples prepared in similar conditions. After isolation on column, solution with proteins was concentrated (usually to a volume of 1 ml and concentration from 150 to 250  $\mu\text{M}$ ) and kept on temperature of  $-80^\circ\text{C}$ ; also in Tris, pH 8.

## 2.3. Optical spectroscopy

### 2.3.1 Theory

Attenuation (loss of intensity) of light that passes through a sample can be used to detect a presence of a chemical substance or macromolecule – this is the basis of optical spectroscopy. Attenuation is measured by absorbance, which is expressed as a common logarithm of the ratio of received to transmitted radiation intensity (eq. 1).

$$A = \log_{10}(I_i/I_f) = \log_{10} T \quad (1)$$

In optical spectroscopy we observe attenuation caused by absorption, but in general it can also be

caused by reflection, scattering, and other physical processes. Absorbance is proportional to concentration and extinction coefficient - all of which are related by Beer-Lambert law (eq. 2). This law states that for N different types of light-absorbing substances in the sample, absorbance is given as:

$$A = \sum_{i=1}^N \epsilon_i \int_0^l c_i(z) dz \quad (2)$$

$\epsilon_i$  is the molar extinction coefficient of the substance  $i$  in the sample, which defines how strongly a given substance absorbs light at particular wavelength, per molar concentration.  $c_i$  is the molar concentration of the substance  $i$  in the sample and  $l$  is the length (in centimeters) through which the beam of light travels in the sample. When there is only one attenuating substance in the sample, and when the sample container is 1 cm wide (which is the standard cuvette size), absorbance can be written as:

$$A = \epsilon c \quad (3)$$

Usually there are two modes of operation of spectrophotometers. First, sample can be scanned with light which wavelength is within a desired range, and the resultant spectra will show absorption intensity as a function of wavelength. Second, sample can be viewed under just one particular wavelength, but within a time period. This is called time-resolved optical spectroscopy and it allows us to observe dynamic processes. Spectra obtained in this way will show changes in absorbance at a particular wavelength as a function of time.

### 2.3.2. Concentration measurements

Unlike most other proteins, hemoproteins are not transparent to visible light and their absorption strongly depends on the oxidation state of certain cofactors - for example, hemes have higher absorbance when they are reduced [10].

We used absorbance of visible light by hemes as a simple way of estimating cytochrome  $bc_1$  concentration [11]. First, reference measurement was taken with just the buffer (100  $\mu$ l) in a cuvette. Then 1-5  $\mu$ l of protein was added and the spectra was recorded with just the protein in the buffer, then after the addition of potassium ferricyanide and after subsequent addition of ascorbate. Potassium ferricyanide oxidises all hemes in the sample and ascorbate reduces cytochrome  $c$  [12],

but not hemes b and heme c<sub>1</sub> because they have lower potential than ascorbate. To fully reduce all hemes, sodium dithionite can be added. Final concentration of cytochrome bc<sub>1</sub> monomers was calculated (in μM) from equation (4) as:

$$c = \frac{A}{\varepsilon} \quad (4)$$

where  $A = (A_{553} - A_{542})_{\text{reduced}} - (A_{553} - A_{542})_{\text{oxidized}}$  represents the difference in absorbances between reduced and oxidized hemes, and  $\varepsilon = 20 \text{ mM}^{-1}\text{cm}^{-1}$  is an extinction coefficient for cytochrome bc<sub>1</sub> [13]. This method can only be used when samples are diluted enough for absorbance never to be higher than 1 - in this region absorbance is linearly dependent on concentration. All of the measurements were done at room temperature. Since this method has a slight margin of error, usually the average of three such measurements was taken.

### 2.3.3. Protein activity measurements

Cytochrome bc<sub>1</sub> enzymatic activity was measured by observing reduction rate of cytochrome c. This was done by adding DBH<sub>2</sub> (water soluble QH<sub>2</sub> analogue) and horse-heart cytochrome c to isolated protein. After the addition of DBH<sub>2</sub> cytochrome bc<sub>1</sub> starts reducing cytochrome c, which is in the beginning completely oxidized. The reduction of cytochrome c was followed by measuring absorbance at 550 nm. Turnover rates (reduction rates of cytochrome c) were calculated from the initial points of the kinetic curves where the time dependence of cytochrome c reduction is linear, taking protein concentration into account [14]. This was performed in Tris buffer with pH 8.

### 2.3.4. Reactive oxygen species (ROS) production measurements

Even at saturating concentrations of antimycin, with all of the Q<sub>i</sub> sites in the cytochrome bc<sub>1</sub> in a sample blocked, reduction of cytochrome c is still not completely inhibited [15]. This is because bc<sub>1</sub> can still perform one turnover when antimycin is present and hemes b are oxidized, but now electrons go from hemes b back to Q or SQ in the Q<sub>o</sub> site. From there, they can go to high potential chain and reduce cytochrome c – this is possible when iron-sulphur cluster is close to Q<sub>o</sub> site and oxidized. Alternatively, when iron-sulphur cluster is far from Q<sub>o</sub> site, electrons can either transfer

directly from SQ to cytochrome c, or react with O<sub>2</sub> to create superoxides (also known as reactive oxygen species, ROS), which in turn reduce cytochrome c non-enzymatically [16].

We can distinguish between enzymatic and non-enzymatic reduction of cytochrome c by adding superoxide dismutase (SOD) which relays the electron from superoxide to hydrogen peroxide (H<sub>2</sub>O<sub>2</sub>) instead of cytochrome c [17]. If rate of cytochrome c reduction decreases after addition of SOD, then we know cytochrome c was reduced non-enzymatically and we know we have superoxides in the sample produced by cytochrome bc<sub>1</sub>.

## **2.4. Flash activated electron transfer in chromatophores**

### **2.4.1. Theory**

This experimental technique is a type of optical spectroscopy, also based on measuring the absorbance properties of a sample. Here, there are two beams of light of different wavelengths aimed at the sample, and the resultant spectra is the difference between absorbance at those two wavelengths. This kind of device is called dual wavelength spectrophotometer. The wavelengths have to be manually set for every experiment, meaning that we cannot scan the sample over the range of wavelengths. This is a time-resolved spectroscopy and as such allows us to monitor dynamics of redox reactions.

This technique takes advantage of fact that chromatophores obtained from *R. capsulatus* (in process mentioned before) contain functional components of photosynthetic pathway: photosynthetic reaction centres, cytochrome bc<sub>1</sub> and cytochrome c. When excited by light, the reaction centres reduce Q to QH<sub>2</sub> and oxidise cytochrome c, resupplying the quinone pool with electrons and protons. This QH<sub>2</sub> then binds to cytochrome bc<sub>1</sub> and starts forward or reverse reaction, reducing the hemes. Because the absorption of hemes depends on their oxidation state, this mechanism allows precise monitoring of the rate and intensity of their reduction and oxidation.

Regeneration of QH<sub>2</sub> and oxidised cytochrome c is possible because photosynthetic pathway is cyclic, and this allows us to take repeated measurements with the same sample. To stimulate photosynthetic reaction centres a flashlight is used, as reflected in the name of the technique.

## 2.4.2. Experimental procedure

Mediators (2.5  $\mu$ l of DAD, 2  $\mu$ l of NQ, 2  $\mu$ l of HNQ, 1  $\mu$ l of PES and 1  $\mu$ l of PMS; full names in materials) and valinomycin (1  $\mu$ l) were added to 7 ml of Tris buffer in a cuvette. Mediators, some of which are water-soluble and some of which are soluble in fatty acids, act as electron acceptors and donors and catalyse the potential equilibration between the electrode and the redox centres (hemes). They are convenient for this experiment because they all lack optical interference in the 500 - 600 nm region. Valinomycin destroys the existing membrane potential before the experiment by transporting potassium ions through lipid membranes, but does not affect proton concentration (pH) [18].

After addition of valinomycin and mediators, cuvette was placed under argon to remove oxygen from the buffer, to avoid creating reactive oxygen species in the sample. After few minutes, when buffer is oxygen-free, chromatophores are added to the buffer, electrode is placed in a cuvette and the system is sealed, with argon still flowing in and out of the sample. In order to prevent oxygen from coming into the cuvette, inhibitors, potassium ferricyanide and sodium dithionite were added to the sample with syringes. Sample was constantly stirred with magnetic stirrer to keep the potential at constant level, except when taking measurements. All of the measurements were done at room temperature and in the dark so as not to simulate reaction centres.

Unlike isolated protein, the concentration of chromatophores was not determined before the experiments. To be able to compare results from flash experiments made on different batches of chromatophores, at the start of every experiment absorbance profile of reactions centres was obtained, the amplitudes of which are proportional to concentrations. Those were taken at differential wavelengths of 603 – 540 nm and at ambient redox potential of 380 mV (maximum of adsorption for reaction centres is at that potential, regardless of the pH) [19].

## 2.5. Electron paramagnetic resonance spectroscopy

### 2.5.1. Theory

Electron paramagnetic resonance (EPR) spectroscopy is based on the fact that unpaired electrons are able to absorb electromagnetic radiation when exposed to external magnetic field, and that absorption is dependent on molecular environment of the electron. Organic compounds with unpaired electrons are usually of special interest in biochemistry, for example free radicals, or hemes and other metal complexes which in some forms have an unpaired electron and which are often crucial for enzyme function.

Basis of this technique is the electronic Zeeman effect. In the absence of external magnetic field, all unpaired electrons in molecules of the same type have equal energy. However, when the sample is exposed to magnetic field  $B$  the energy levels are split. This is due to the fact that electrons, being fermions, can have spins (intrinsic magnetic moments) with two different orientations in respect to the magnetic field,  $+1/2$  and  $-1/2$   $\hbar$  (where  $\hbar$  is the reduced Planck constant), and when those spins interact with the external magnetic field  $B$  the electron energy level increases or decreases.

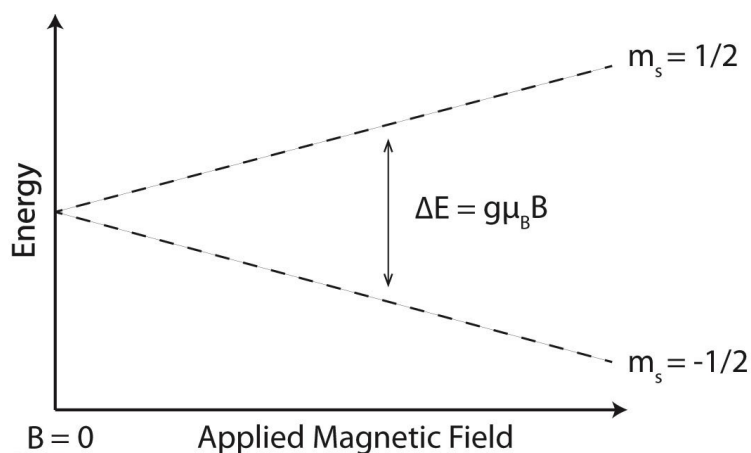


Figure 7: Zeeman effect - splitting of electron energy levels in external magnetic field.

The difference in energy levels is a linear function of magnetic field  $B$ :

$$\Delta E = g\mu B \quad (5)$$

where  $g$  and  $\mu$  are constants, Bohr magneton and Lande  $g$ -factor, respectively.

While the system is in thermal equilibrium (no net energy input) populations on those energy levels follow the Boltzmann distribution:

$$\frac{n_1}{n_0} = \exp\left(\frac{-\Delta E}{kT}\right) \quad (6)$$

where  $n_1$  and  $n_0$  are populations on higher and lower energy level (or in different terminology, excited and ground state),  $k$  is Boltzmann's constant,  $T$  is the temperature and  $\Delta E$  is the difference in energy of the states.

While the EPR sample is in the magnetic field, it is simultaneously exposed to electromagnetic radiation which gives electrons energy to jump from ground to excited state. We can see from equation (5) that the stronger the magnetic field  $B$  is, the bigger the difference in energy levels of electrons. At certain  $B$  values, difference between the two electron energy levels matches the energy of the incoming radiation. This is where the transition between the states is at its peak, and electronic spins resonate with the electromagnetic radiation.

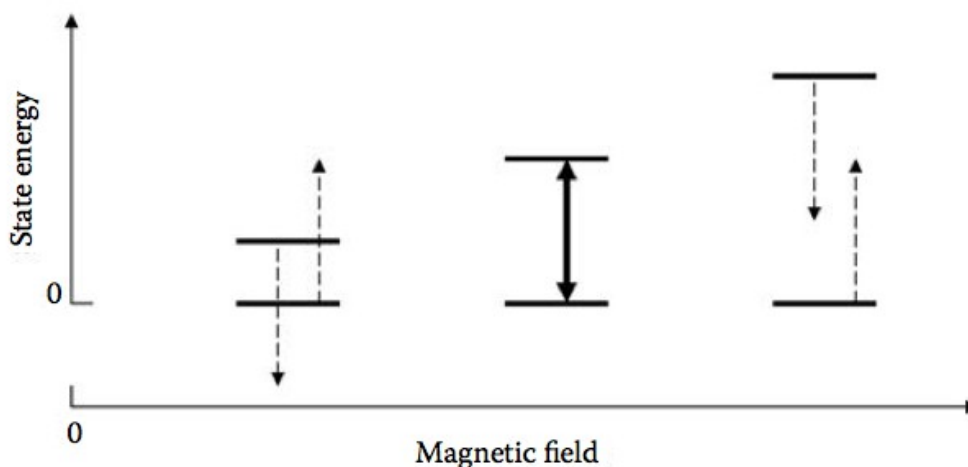


Figure 8: energy states split by the magnetic field. The middle scheme represents resonance condition.

Since there are initially more electrons in the ground state than in the excited state, as dictated by the Boltzmann distribution, this resonance will lead to net absorption of energy. It is this absorbance that is detected in the EPR device, but it is more common to show first derivative of the EPR spectra (fig. 9).

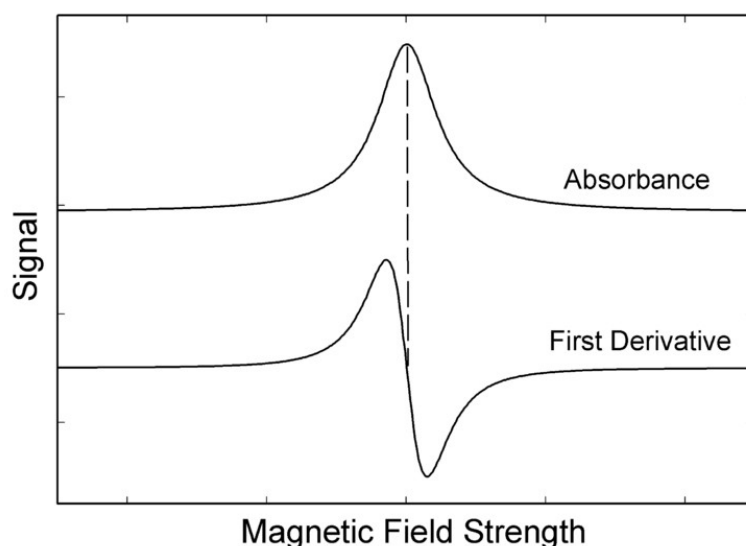


Figure 9: absorbance profile and its first derivative.

Knowing that the energy of electromagnetic radiation is:

$$E = h\nu \quad (7)$$

and that the energy difference between two levels is as described by equation (5), the condition for EPR resonance can be written as:

$$h\nu = g\mu B \quad (8)$$

where  $h$  and  $\mu$  are Planck's constant and Bohr magneton, respectively.  $g$  is Lande  $g$ -factor, the value which reflects spin-orbit coupling of the electron and is in general dependent of the chemical environment of the paramagnetic centre. For example,  $g$  value of of metal-ion complex will change in the presence of ion nucleus. We can rewrite equation (8) as:

$$g = \frac{h\nu}{\mu B} \quad (9)$$

From this we can see that, knowing the wavelength  $\nu$  and magnetic field strength  $B$ , we can calculate electronic  $g$  factor. This is the main idea behind EPR, this is what allows us to probe the molecular environment.  $g$  value of a free electron in vacuum is 2.00232; for organic radicals the variation is very small, usually with values ranging from 1.99 – 2.01, while for transition metal complexes it can range from 1.2 – 3.8 [20].



Zeeman interactions are in general anisotropic and depend on the orientation of paramagnetic centre in respect to the external magnetic field. This anisotropy comes from immediate surroundings of the atom with an unpaired electron. This means that in general there is not just one single  $g$  value, but instead that  $g$  is represented by a 3x3 matrix with 3 principal values:  $g_x$ ,  $g_y$  and  $g_z$ . Paramagnetic centre can be either isotropic, with one  $g$  value ( $g_x = g_y = g_z$ ), axial ( $g_x = g_y \neq g_z$ ), or rhombic ( $g_x \neq g_y \neq g_z$ ). For example, hemes are usually rhombic, with four nitrogens in a plane and at equal distance from the iron in the centre (meaning that  $g_x = g_y$ ) and the axial ligands below and above the plane (producing a  $g_z$  value different from  $g_x = g_y$ ).  $g$  anisotropy is not detectable in fluid solution, where the molecules rapidly tumble and the measured  $g$  value is average over all molecular orientations, but can be readily observed in powder or frozen sample.

In most EPR setups the electromagnetic radiation is kept at constant wavelength, while  $B$  is varied. This is in contrast to other magnetic spectroscopic techniques such as NMR, where  $B$  is kept constant and the frequency of the radiation is changed. The reason for this is that the wavelength needs to correspond to dimensions of the cavity in which sample is held, and so cannot be changed. The dimensions of the cavity are adjusted to maximize the magnetic component of electromagnetic wave and minimize the electric component, in order to minimize non-resonant (nonspecific) adsorption and increase signal to noise ratio.

While both resolution and sensitivity increase with increasing frequency, magnetic field required to achieve resonance is also greater and at certain point becomes experimentally unpractical. The optimum of sensitivity versus magnetic field strength is at microwave frequencies of 9 - 10 GHz, corresponding to wavelength of around 30 mm. This is called X-band frequency and it is the most common frequency used in EPR. For a resonance frequency of 9.500 GHz (9500 MHz) and a  $g$ -value of 2.00232 the resonance field is 0.338987 Tesla (3389.87 Gauss) [20].

Because of the great difference between masses of electrons and nucleons, magnetic moment that arises from interaction between electrons and external magnetic field is much larger than the one from nucleons. Consequently, at given magnetic field strength, much higher electromagnetic frequency is required to induce spin resonance with electrons than with nucleons, so there is no overlapping between EPR and NMR signals.

Energy absorbed by the electrons can be released into the system through spin-lattice relaxation. Lattice is term for anything that surrounds the electron we observe, which in this experiments was the protein solution. Spin-lattice relaxation time is the constant related to the recovery of the electron spin magnetization component parallel to external magnetic field, towards its thermal equilibrium value. It is important because it can provide information about molecular surroundings of the paramagnetic centre. Specifically, relaxation time  $T$  is the time in which the spin system loses  $e^{-t/T}$  of its excess energy. Spin-lattice relaxation is what permits us to take repetitive measurements – otherwise, all the electrons would stay in excited state and system wouldn't be able to absorb any more energy.

We can assess the relaxation time of a paramagnetic centre by a method called power saturation. Due to equipment-related factors which determine how effectively microwaves affect paramagnetic centre, it is rather hard to determine the precise value of relaxation time in this method. This is why usually relaxation properties of different paramagnetic centres are instead compared to one another, given that the power saturation experiments are performed in the same resonator and on the same temperature.

When exposed to radiation of low power, electron spins are not saturated – they can absorb most of the microwave energy and effectively release it back to the system through spin-lattice relaxation. In this conditions EPR signal strength is proportional to the square root of power. However, as we apply higher microwave power the sample becomes saturated. Now the relaxation rate is not fast enough to dissipate the energy being absorbed and to bring back the Boltzmann distribution of states, and so the amplitude of EPR spectrum drops. In extreme case, when we put a lot of energy into the sample, the populations of ground and excited state become equal and we observe no signal. Spins with slower relaxation rates exhibit saturation in lower power than those with faster relaxation rates, which is why we can assess the relaxation time by power saturation .

## **2.5.2. Experimental procedure**

The reason why we observe SQ in EPR is that it is in fact the only form of quinone detectable by EPR, since only SQ has a single unpaired electron. Signal from SQ in cytochrome  $bc_1$  is barely detectable in room temperature, but much larger in frozen samples. However, this is not simply the result of change in population ratio in Boltzmann distribution (eq. 6), because this is not enough to

account for the great difference between signal amplitudes on different temperatures. It is speculated that this higher signal is caused by stopping the movement of SQ in frozen samples, arresting the SQ in the Qi site. The mutations in cytochrome bc<sub>1</sub> mutants we used were designed to mimic this freezing.

Apart from getting better SQ signal, one more reason to view frozen samples is that rates of chemical reactions are then stopped completely, which allows us to observe even radicals that are unstable on room temperatures. If prepared correctly, for example with glycerol, most biological macromolecules can be frozen and heated up repeatedly without the loss of biological function.

Samples were prepared in EPR tubes and frozen immediately after preparation. They were frozen and kept in liquid nitrogen. Volume of all samples was around 140 µl due to small volume of EPR tubes, which are very narrow (up to 4 mm) in order to fit into EPR spectrometer. Reactants were always added in such amount that their final concentration in the sample was 20 µM of protein, 40 – 100 µM of DBH<sub>2</sub> (2-5 times higher concentration than that of the protein), 40 – 100 µM of myxothiazol and 40 – 100 µM of antimycin.

Potentiometric titration of chromatophores was done in an experimental setting similar to that for flash-induced spectroscopy – in oxygen-free environment (in argon), at room temperature and in the dark. One difference is that here chromatophores were not diluted in buffer, in order to have them highly concentrated. The redox potential of chromatophores was first brought to highest desired point using potassium ferricyanide and then gradually lowered with sodium dithionite, with samples taken at desired intervals. EPR tubes in which the samples are put were also kept in argon and the sample was frozen immediately after preparation. Mediators used were QH, DAD, NQS, NQ, DQ, HNQ, AQS, PMS, PES and ITS (full names in materials).

All EPR and flash spectroscopy data was processed using ELEANA software, available at <http://larida.pl/eleana/>

### 3. Results and discussion

#### 3.1 Optical spectroscopy measurements

Optical spectroscopy was used to confirm the presence of  $bc_1$  in a solution, measure its concentration and to check if protein preparation was successful and if protein subunits containing hemes  $b_H$ ,  $b_L$  and  $c_1$  are present. It was also used to obtain absorbance profile of both mutants and compare them to that of wild type (fig. 10), to check if we can use the same range of wavelengths to observe all samples in flash spectroscopy experiments. Samples were viewed in wavelength range of 500 nm to 700 nm. While with optical spectroscopy we can distinguish between heme c and hemes b, we cannot distinguish between hemes  $b_H$  and  $b_L$ , which both have maximum of absorption at 551 nm.

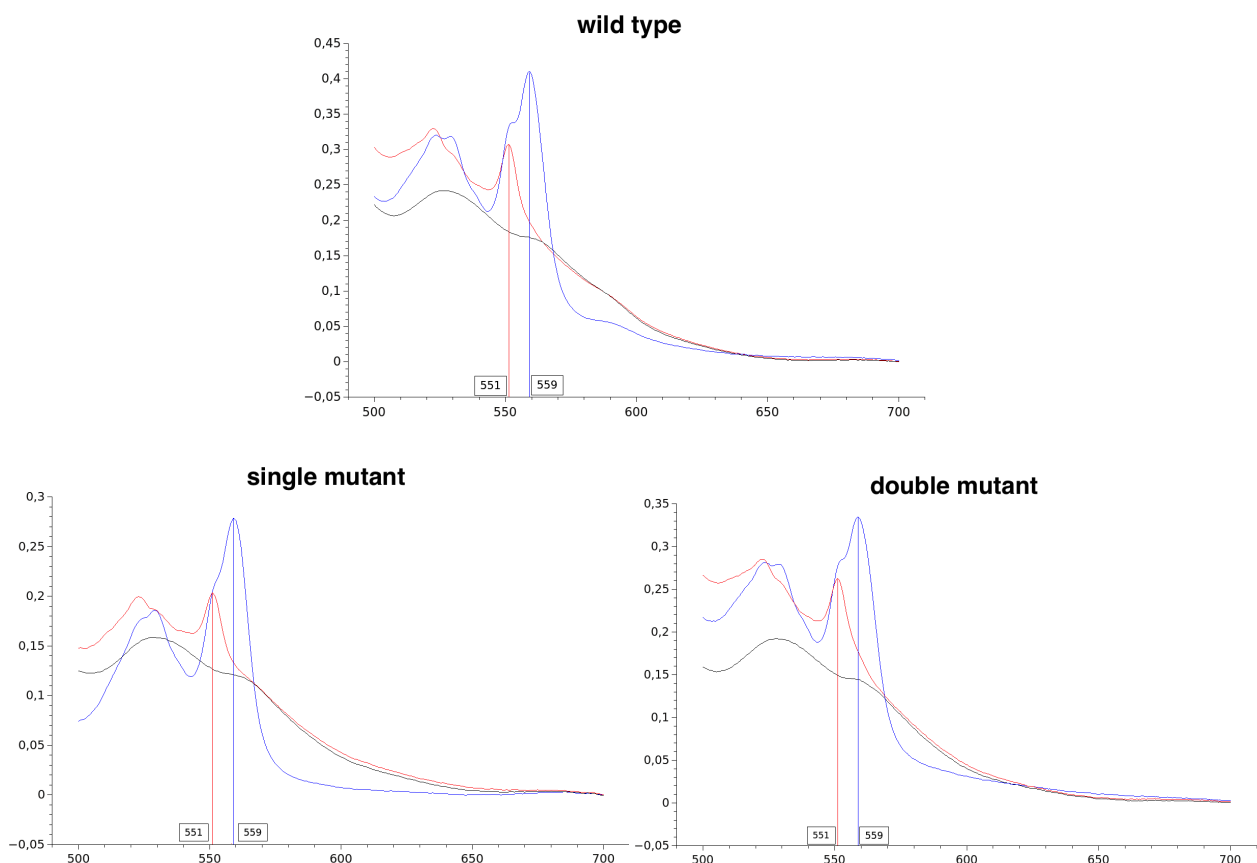


Figure 10: adsorption profiles of wild type (WT), single mutant (SM) and double mutant (DM). x-axis is wavelength (in nm) and y-axis is absorbance (in arbitrary units). We can see that both mutants have similar adsorption profiles as wild type, with maximum of adsorption for hemes b and heme c in the same wavelength as wild type, 551 nm and 559 nm respectively. Hemes were oxidized by adding potassium ferricyanide (red traces) and reduced by adding sodium dithionite (blue traces).

Optical spectroscopy was also used to determine the enzymatic activity, which is the reduction rate of cytochrome c by cytochrome bc<sub>1</sub> in steady-state conditions (with high excess of cytochrome c over cytochrome bc<sub>1</sub>). Enzymatic activity of double mutant was measured to be 109.84 s<sup>-1</sup>, approximately three times lower than that of wild type, which is around 330 s<sup>-1</sup>[21].

### 3.2. Flash spectroscopy measurements

Flash spectroscopy was used to observe forward and reverse reaction in mutants and wild type. Forward reactions were measured in pH 7 and 9, and reverse reactions just in pH 9 because the reaction rate in pH 7 is too small to detect. In pH 7, measurements were taken at ambient redox potential of 100 mV and 200 mV, and in pH 9 in -20mV and 250 mV. In pH 7 quinone pool is half oxidized and half reduced, and in pH 9 more than half of quinone are oxidized. This means there is less quinone available to be oxidized by the cytochrome bc<sub>1</sub>, which is why signal amplitude is lower in pH 9. Every trace shown here is an average over 6 consecutive measurements, in order to increase signal to noise ratio. Hemes b were viewed at differential wavelengths of 560 – 570 nm and hemes c at 550 – 540 nm. All of the traces are scaled to be comparable, based on amplitudes of their respective reaction centre traces. For all samples, measurements were taken before the addition of inhibitor, with just one inhibitor and after addition of both inhibitors. In kinetic profiles obtained from flash experiments, higher signal amplitude (stronger absorbance) means that larger percentage of hemes is reduced. We were primarily interested in reverse reaction rates because then Qi site SQ is produced in large quantities and so EPR signal of SQ is higher in those conditions.

In figure 11 we can see comparison of forward reactions (QH<sub>2</sub> binding to Qo site) on hemes b in wild type, single mutant and double mutant. Green traces are without any inhibitors, red traces are after addition of antimycin and black traces are with both antimycin and myxothiazol. Amplitude is in arbitrary units. All of the experiments were performed on room temperature, at pH 7 and measured at ambient potential of 100 mV. This conditions were chosen for comparison because they represent conditions in bacterial cell. The amplitude represents difference between absorbance measured at 560 and 570 nm.

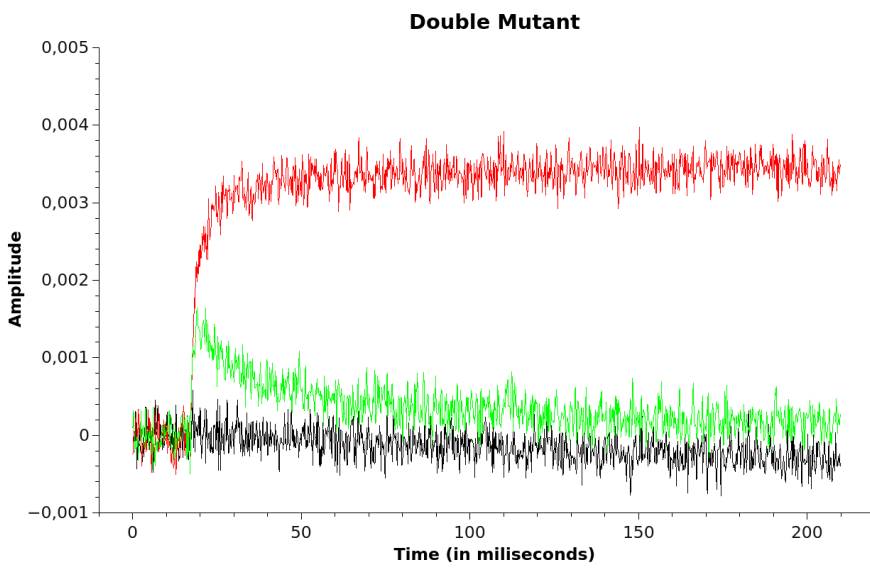
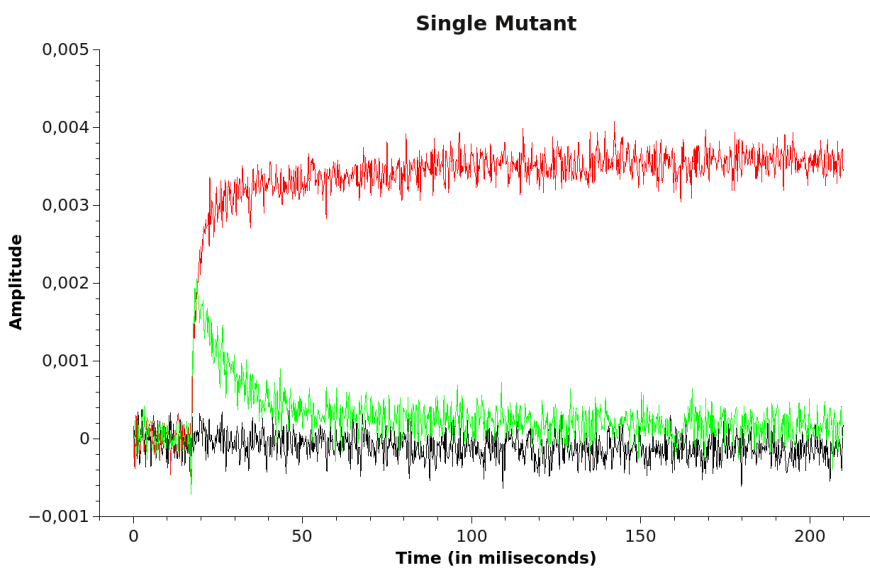
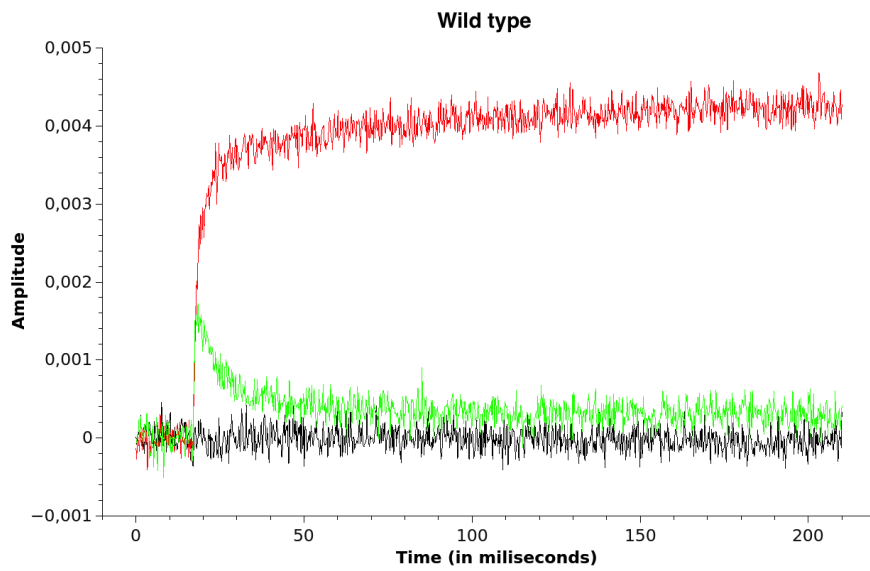


Figure 11

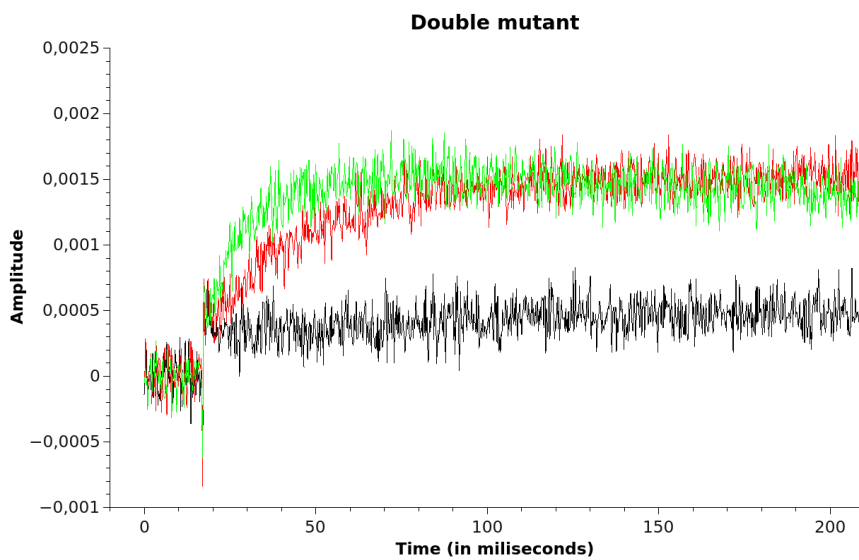
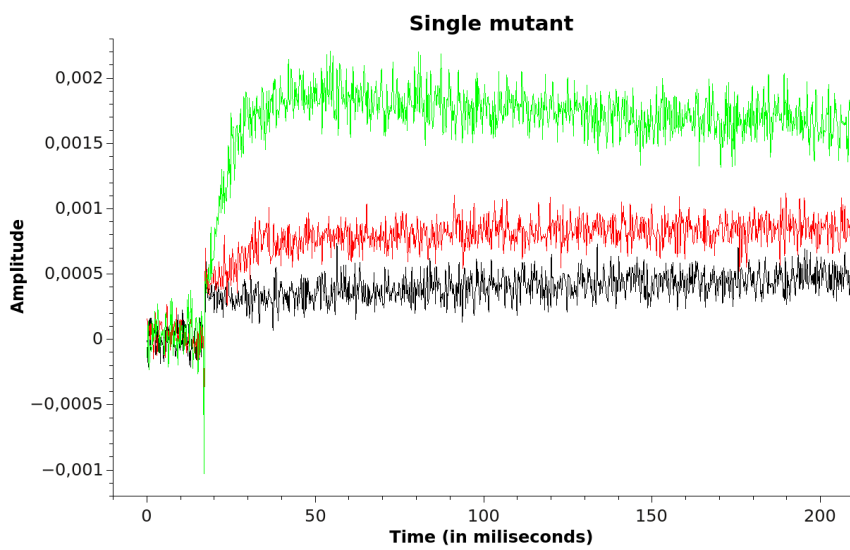
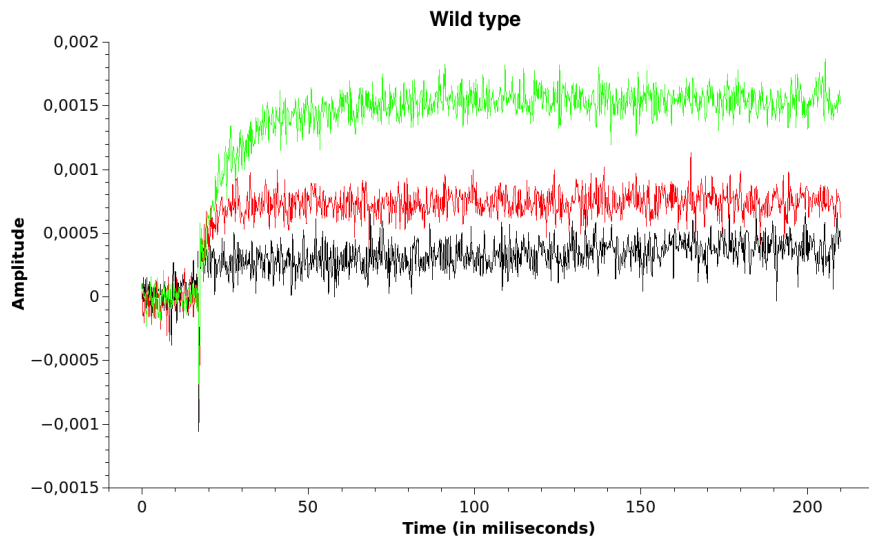


Figure 12

In figure 12 we can see comparison of forward and reverse reactions on both mutants and wild type, obtained using flash-induced optical spectroscopy. Green traces represent signals from hemes  $b_H$  with no inhibitors present (primarily forward reaction,  $QH_2$  binding to  $Q_o$  site), red with myxothiazol (forward reaction blocked,  $QH_2$  binding to  $Q_i$  site), and black with both myxothiazol and antimycin (no reaction). Amplitude is in arbitrary units. All of the experiments were performed on room temperature, at pH 9 and measured at ambient potential of 250 mV. The amplitude represents difference between absorbance measured at 560 and 570 nm.

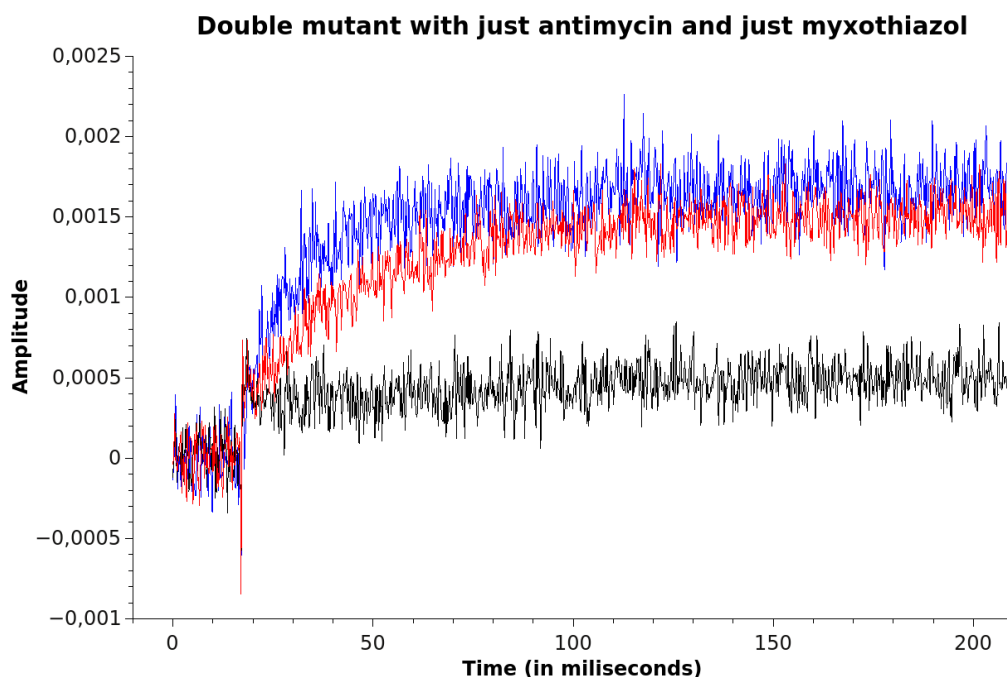


Figure 13: As in fig. 12, red trace represents sample with just myxothiazol (forward reaction blocked,  $QH_2$  binding to  $Q_i$  site), and black with both myxothiazol and antimycin (no reaction). Blue trace is signal from hemes  $b_H$  with just antimycin present (just forward reaction). Amplitude is in arbitrary units. Spectre was recorded on room temperature, at pH 9 and measured at ambient potential of 250 mV. The amplitude represents difference between absorbance measured at 560 and 570 nm.

We were primarily interested in reverse reaction rates because SQ in  $Q_i$  site is produced in large quantities during reverse reaction and so its EPR signal is higher in those conditions. Forward reactions on hemes  $b$  (fig. 11) serve to confirm that reaction rates are comparable on all mutants. On the other hand, the amplitude of reverse reaction in double mutant is much larger than in single and wild type (red traces), comparable to forward reaction for the same mutant (fig. 13). This indicates that more hemes  $b_H$  get reduced in double mutant than in wild type.



### 3.3. EPR measurements of semiquinone

We proceeded to measure SQ signal on EPR. This was done on isolated complexes of cytochrome  $bc_1$ , on temperatures of 200 K. Those measurements unexpectedly show no SQ signal for double mutant and only small signal in single mutant compared to wild type (fig. 14). This was also not in accordance with results from flash-spectroscopy, since we expected higher SQ signal because the amplitude of reverse reaction (heme  $b_H$  reduction) was higher in double mutant – we observed that, on average, more electrons went to b chain, so we expected that more SQ should accumulate in  $Q_i$  site.

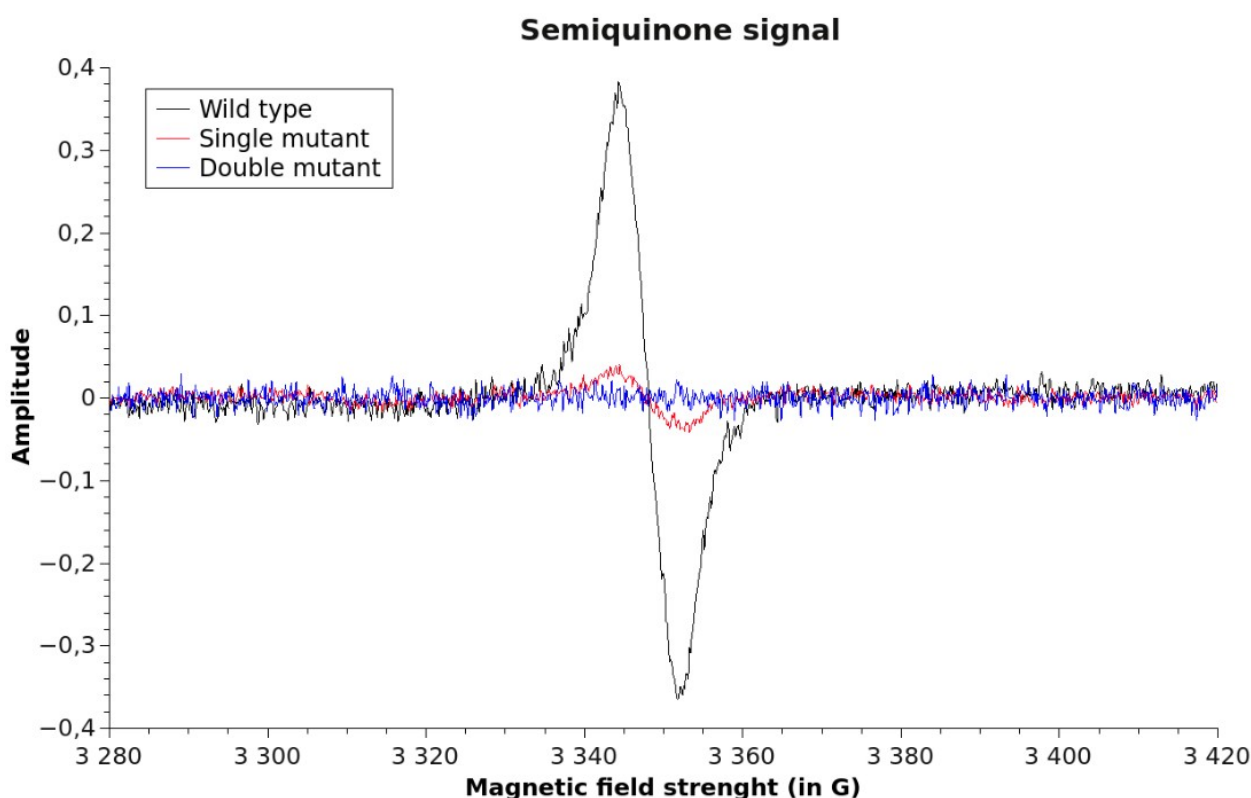


Figure 14: EPR signal of SQ induced in  $Q_i$  site of cytochrome  $bc_1$ , after addition of myxothiazol and  $DBH_2$ . Amplitude is in arbitrary units. Spectra were recorded at 200K, with power of 5 mW, modulation amplitude of 3 G and at X-band (microwave frequency 9.390)

Only when the  $g$  anisotropy is big do we observe spectra with three resolved transitions corresponding to  $g_x$ ,  $g_y$  and  $g_z$  values. However, in case of SQ the  $g$ -anisotropy is very small and so when we use lower frequency (X-band) those  $g$  values are very close to each other. This is why we only see one transition here.

We can see that both single mutant and wild type have maximum of adsorption at  $B = 3348.125$  Gauss, which is  $0.3348125$  Tesla (an SI unit). Knowing that microwave frequency used was  $9.390$  GHz, that Planck's constant is  $h = 6.626 \times 10^{-34} \text{ m}^2 \text{ kg s}^{-1}$  and Bohr magneton is  $\mu_B = 9.274 \times 10^{-24}$ , we can calculate the value of Lande g-factor corresponding to the SQ line position using the equation (9) as:

$$g = ( 6.626 \times 10^{-34} \text{ J s} * 9.390 \times 10^9 \text{ s}^{-1} ) / ( 0.3348125 \text{ T} * 9.274 \times 10^{-24} \text{ J T}^{-1} ) = 2.003772$$

This is close to the reported g value for SQ at the Qi site of  $2.0048$ . [22]

### **3.4. Power saturation**

We also performed SQ power saturation experiments. Again, there was no signal for double mutant, so only results from single mutant and wild type are shown here (fig. 15 and 16). Each sample was measured at 17 different power levels (only 13 of each are shown in figure 15).

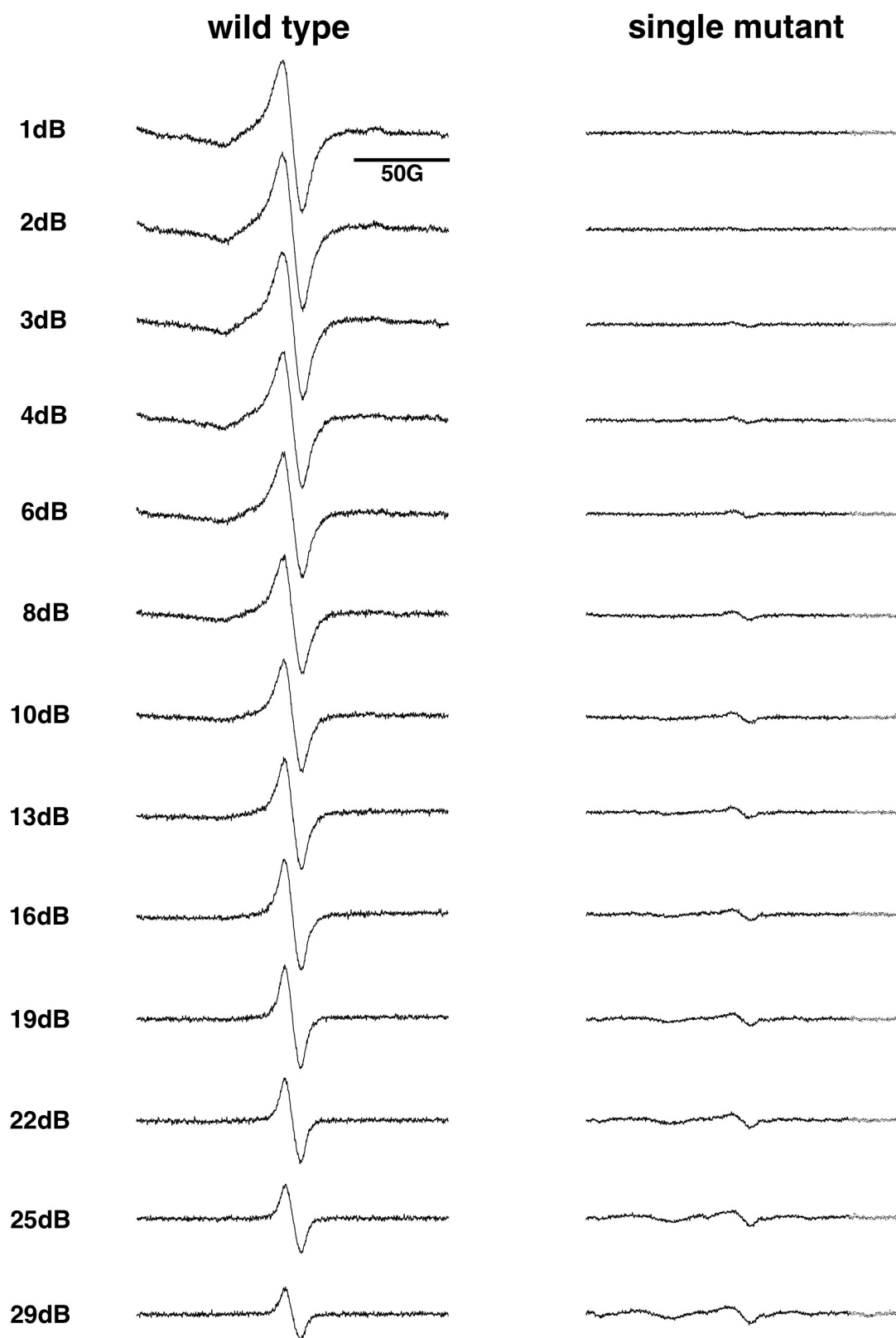


Figure 15: Signals on the left are from wild type and on the right from single mutant. Signals are in order of increasing attenuation (decreasing power). Spectra were recorded at 200K, with variable power (maximum power is 200 mW at 0 dB attenuation), modulation amplitude of 3 G and at X-band (microwave frequency 9.390). All signals are in range from 3280 G to 3420 G, same as in figure 14.

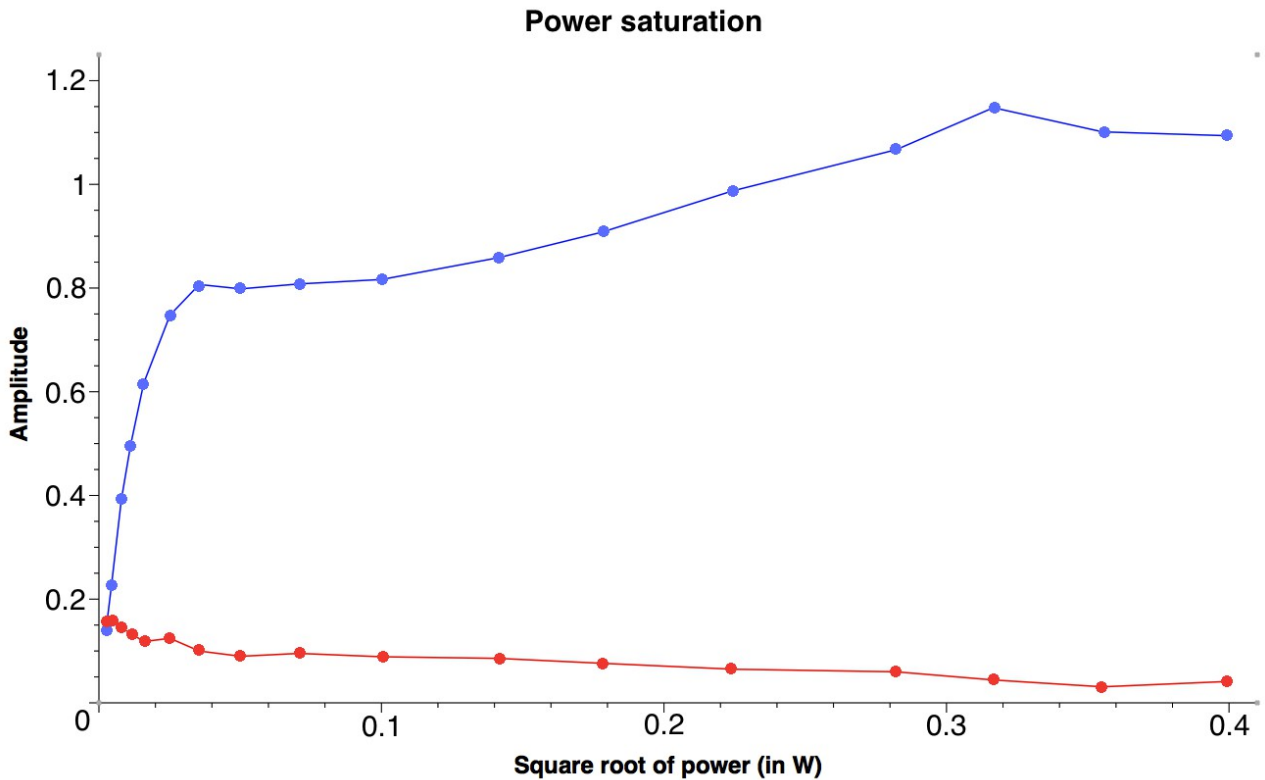


Figure 16: SQ signal amplitude vs. square root of power (maximum power was 200 mW at 0 dB attenuation). Blue trace is wild type, red is single mutant.

Power saturation data is standardly shown as signal amplitude vs. square root of power. Standard power saturation curve reaches maximum and then signal decreases almost to zero. Wild type SQ signal observed here instead follows a non-standard power saturation curve. This is because here we have two components of the curve – one saturating and one non-saturating [23]. The non-saturating component indicates there is a fast relaxing paramagnetic SQ species in wild type cytochrome  $bc_1$ .

Single mutant SQ signal is, however, quite strange and does not follow neither standard nor two-component power-saturation plot shape. Reason for this might be that signal is generally weak (as seen in fig. 14) and thus other background signals are comparable to it and they overlap (presence of other signals can be visible in lower right in figure 15). This means signal from single mutant is unreliable for this kind of measurements.

### 3.5. Potentiometric titration of semiquinone

At this point we decided to focus on double mutant, to see if we can detect SQ signal in it. We tried raising the concentrations of both myxothiazol and DBH<sub>2</sub> in an EPR sample to 100  $\mu$ M and leaving the sample on room temperature for several minutes after mixing, before freezing in liquid nitrogen, but none of those approaches yielded results.

To see if SQ signal perhaps depends on ambient redox potential, potentiometric titration of SQ in double mutant and wild type was performed. This was done on chromatophores, not isolated protein, to also check if using DBH<sub>2</sub> instead of native QH<sub>2</sub> is responsible for lower or no SQ signal in mutants. In figure 17, left, we can see the presence of SQ in wild type when there are no inhibitors, with peak production of SQ (strongest reverse reaction) in redox potential around 40 mV and the absence of signal from SQ in Qi site when antimycin was applied, as expected. On double mutant however, SQ was not observed at all (fig. 17, right). This is consistent with results from EPR measurements of isolated complexes, confirming there is no SQ signal in double mutant on any potential. The signal amplitude is above zero even with antimycin in both mutants since in chromatophores there is also SQ from other proteins, so there is always some background SQ signal present [24].

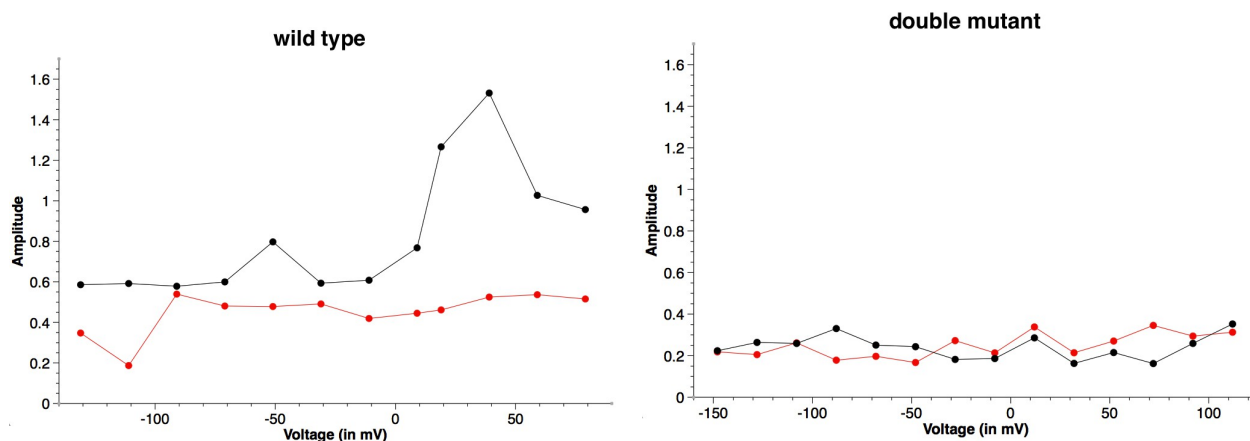


Figure 17: titration samples of SQ in chromatophores. Black trace is with without inhibitors, red trace is with antimycin. Amplitude is in arbitrary units. EPR spectra were recorded at 200K, with power of 0.06 mW for wild type and 0.2 mW for double mutant, modulation amplitude of 6 G and in X-band (microwave frequency 9.390)

### 3.6. EPR measurements of hemes b

The fact that reverse reaction was confirmed by flash-induced spectroscopy yet no SQ could be detected in EPR was somewhat puzzling. One possible explanation for this discrepancy was that not just one, but both electrons from QH<sub>2</sub> go to low potential chain of cytochrome bc<sub>1</sub>, to both hemes b<sub>L</sub> and b<sub>H</sub>, leaving only quinone at the Qi site. To test this, we used EPR to observe both hemes b during reverse reaction. Figure 18, left, shows hemes b EPR spectra in wild type before and after addition of DBH<sub>2</sub> – we can see that after addition of DBH<sub>2</sub>, only heme b<sub>H</sub> gets reduced, meaning that one electron from DBH<sub>2</sub> got transferred and SQ was left at Qi site. Figure 18, right, shows hemes b in double mutant – we can see that, as in wild type, heme b<sub>L</sub> is still oxidized after addition of DBH<sub>2</sub>, but the amplitude of the signal from heme b<sub>H</sub> is higher than in wild type. This is in agreement with results obtained from flash-induced optical spectroscopy (larger amplitude of reverse reaction in double mutant), but still does not explain the lack of SQ EPR signal in double mutant.

In figure 18 we can see EPR spectra of myxothiazol inhibited cytochrome bc<sub>1</sub> before (red trace) and after (black trace) addition of DBH<sub>2</sub>. Oxidized hemes are paramagnetic and hence have a higher signal amplitude than reduced hemes which are diamagnetic. Large signal on the left is from iron impurities in the sample. Unlike SQ EPR signal in previous figures, here we observe only g<sub>z</sub> component of g-factor, because the signal is broadened so g<sub>y</sub> overlaps with other signals and g<sub>x</sub> is beyond detection. Heme b<sub>L</sub> has a g<sub>z</sub> value of 3.774 and heme b<sub>H</sub> a g<sub>z</sub> value of 3.46. Amplitude is in arbitrary units. This spectra were recorded in pH 9 and at 10K, with power of 2 mW, modulation amplitude of 15 G and at X-band (microwave frequency 9.390).

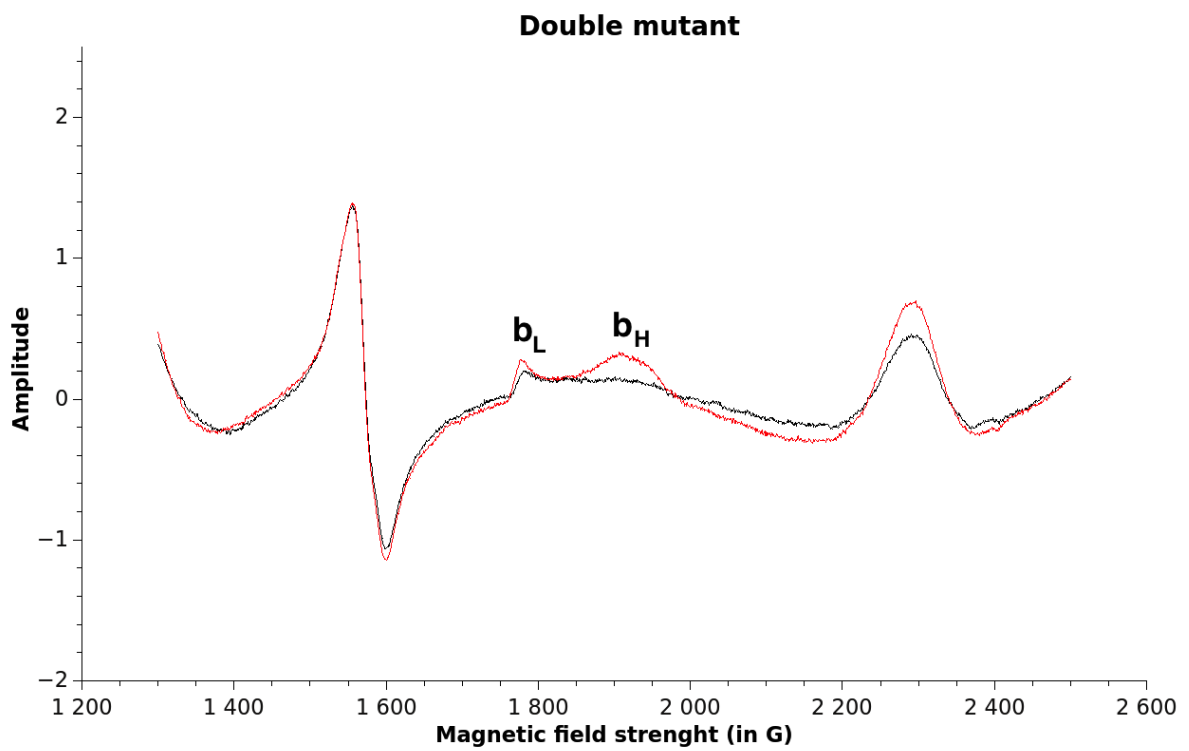
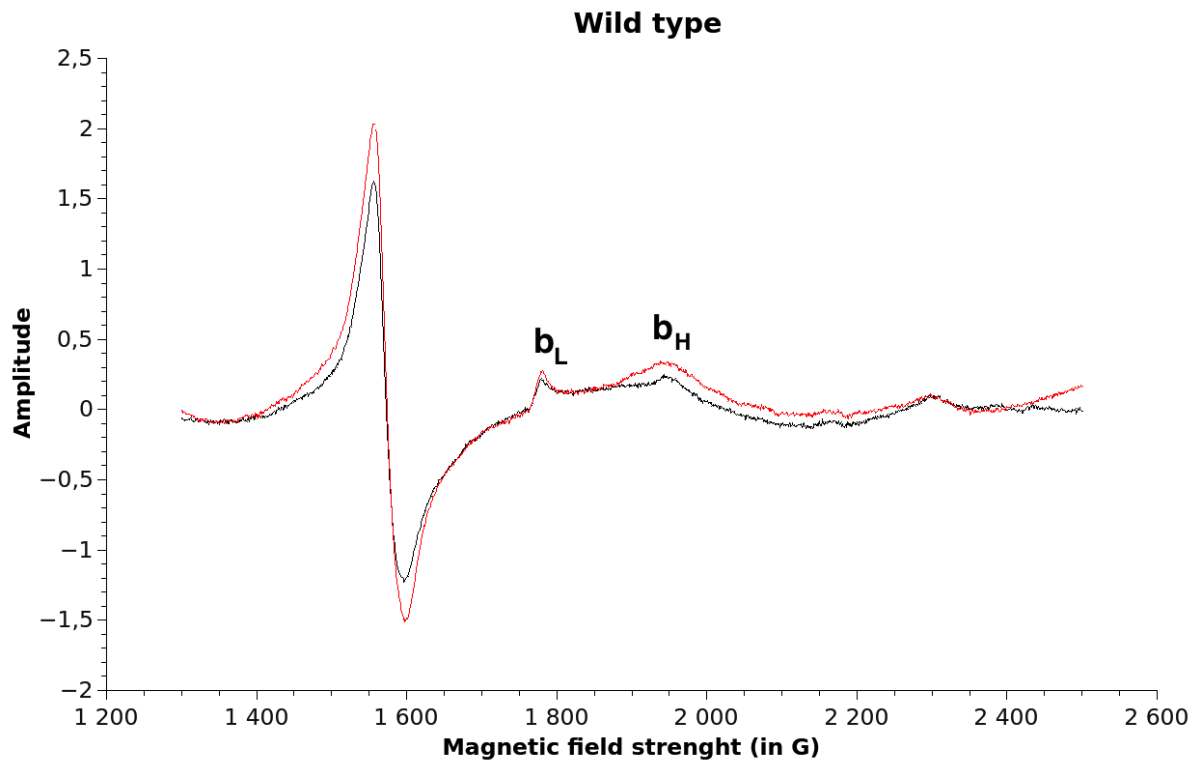


Figure 18

### 3.7. ROS production measurements

Last, we observed superoxide (ROS) production in double mutant. ROS production can happen due to electrons being transferred from SQ formed in the Q<sub>o</sub> site to free oxygen in the environment. To see if something similar happens in Q<sub>i</sub> site of double mutant, ROS production was measured in double mutant and wild type, in isolated protein with myxothiazol and with and without adding superoxide dismutase (SOD).

This was done in same conditions as activity measurements, and turnover rates were also calculated from the initial parts of the absorption spectra curves where the time dependence of cytochrome c reduction is linear.

	Wild type	Double mutant
Without SOD	0.07859	0.2265
With SOD	0.05891	0.1372
ROS production	25%	39.5%

Table 1: comparison of cytochrome c reduction rates in wild type and double mutant. The units are s<sup>-1</sup>

We can see in table 1 that in wild type, adding SOD decreases the amount of cytochrome c reduced by 25%, while in the double mutant it is decreased by 39.5%. This tells us that around 15% more superoxides are produced in double mutant compared to wild type. However, these values are very small compared to standard enzymatic activity, without myxothiazol (0.08 s<sup>-1</sup> compared to 330 s<sup>-1</sup> for wild type and 0.23 s<sup>-1</sup> compared to 100 s<sup>-1</sup> for double mutant) and it is hard to tell if the differences in ROS production in wild type and double mutant are statistically significant.



## 4. Conclusions

Enzymatic activity of the double mutant was measured with optical spectroscopy and was determined to be lower than wild type, but still enough for protein to be able to perform biological function. ROS production measurements indicate that more superoxides are produced in Qi site of double mutant than in wild type, but further measurements would have to be performed for the result to have statistical significance.

Flash spectroscopy shows us that there is stronger reverse reaction in double mutant than in single mutant or wild type. EPR experiments, both on isolated protein and on chromatophores show no SQ signal in double mutant, on any redox potential and regardless of whether we use QH<sub>2</sub> or DBH<sub>2</sub>. EPR observations of hemes b show that more hemes b<sub>H</sub> get reduced in double mutant than in wild type, which is in agreement with flash experiments. Power-saturation experiments done on single mutant were inconclusive – this experimental technique is quite sensitive to noise in the low power regions, and perhaps a higher concentration of proteins is needed for clearer results.

At first we thought that maybe in double mutant larger percentage of cytochromes bc<sub>1</sub> participate in reverse reaction, and so larger percentage of hemes b<sub>H</sub> in a sample are reduced than usual. This would explain results from hemes b<sub>H</sub> in EPR and from flash experiments. However, it doesn't explain why there is no SQ signal in double mutant, and it is highly unlikely given the fact that activity of cytochromes bc<sub>1</sub> in double mutant is much smaller than in wild type.

Second possible explanation for lack SQ signal is that one electron from QH<sub>2</sub> at the Qi site goes to heme b<sub>H</sub>, and the other is transferred to free oxygen and forms superoxides. To test this we performed ROS production measurement and determined that indeed more superoxides are produced in double mutant than in wild type. However, as said before, the activity values are very small and so this result is inconclusive. Even if the result is indicative of the rate of ROS production in double mutant, it might still not be high enough to account for total lack of SQ signal. Also, this wouldn't explain stronger signal from reduced hemes b<sub>H</sub>, unless it happens that both larger percentage of cytochrome bc<sub>1</sub> in a sample participates in reactions and also that free radicals are formed.

Another explanation for this results is that, as cytochrome  $bc_1$  is a dimer, both monomers participate in reverse reaction. It was shown that electrons can go from one heme  $b_L$  to the other; the distance is small enough for them to tunnel. This means there is a possibility that in double mutant one of the electrons goes from heme  $b_H$  of one monomer, through both hemes  $b_L$  to heme  $b_H$  in the other monomer. This kind of inter-monomer electron transfer is also possible in wild type, but it could be that it is more common in double mutant. Important aspect of this pathway could be transfer of electrons from heme  $b_H$  to heme  $b_L$ . It could be that potential of heme  $b_H$  in double mutant is lowered and so the potential gap between hemes  $b_H$  and  $b_L$  is smaller, making it easier for electrons to cross. Although the mutations of single and double mutants were presumed to be far enough from heme  $b_H$  not to affect its potential, this was never confirmed. This would explain both the stronger signal of reduced hems  $b_H$  in flash and in EPR, and the lack of SQ, as both electrons from  $QH_2$  would go to two hems  $b_H$ .

Original goal of this research was to check if it possible to generate SQ in Qi site of cytochrome  $bc_1$  in large amounts at room temperature, using two *R. capsulatus* mutants. However, since we weren't able to observe SQ in double mutant, most of the experiments were aimed at trying to understand why is that so.

Some of the further experiments that could be done to explain the lack of SQ signal are:

- determining the potential of heme  $b_H$  in both double and single mutant
- repeating ROS production measurements in double mutant to get a more reliable data and measuring ROS production in single mutant
- inspecting whether other electron from SQ in Qi site goes to heme  $b_H$  in other part or the dimer, in both single and double mutant
- repeating power saturation experiments for single mutant in different conditions, for example with higher protein concentration

## 5. References

1. Mitchell P.; Protonmotive redox mechanism of the cytochrome bc<sub>1</sub> complex in the respiratory chain: protonmotive ubiquinon cycle; *FESB lett.* 56: 1-6, (1975)
2. Cooley J.W., Darrouzet E. and Daldal F.; Bacterial hydroquinone: cytochrome c oxidoreductases. Physiology, structure and function. In: Respiration in archea and bacteria Vol. 1: Diversity of procaryotic electron transport carriers 41-55, Davide Zannoni (ed), Kluwer Academic Publishers, Dordrecht (2004)
3. Darrouzet E., Moser C.C., Dutton P.L. and Daldal F.; Large scale domain movement in cytochrome bc<sub>1</sub>: a new device for electron transfer in proteins; *Trends Biochem. Sci* 26(7): 445-451 (2001)
4. Osyczka A., Moser C.C., Daldal F. and Dutton P.L.; Reversible redox energy coupling in electron transfer chains; *Nature* 427: 607-612 (2004)
5. Yu L, Tso S.C., Shenoy S.K., Quinn B.N., Xia D.; The role of the supernumerary subunit of Rhodobacter sphaeroides cytochrome bc<sub>1</sub> complex; *J. Bioenerg. Biomembr.* 31(3): 251-257 (1999)
6. Berry E.A., Huang L.S., Saechao L.K. and Pon N.G., Valkova-Valchanova M.B., Daldal F.; X-ray structure of Rhodobacter capsulatus cytochrome bc<sub>1</sub>: comparison with its mitochondrial and chloroplast counterparts; *Photosynth. Res.* 81: 251-275 (2004)
7. Dutton P.L. and Prince R.C.; Reaction-center driven cytochrome interactions in electron and proton translocation and energy coupling. In: The photosynthetic bacteria 525-570, Clayton R. K. and Sistrom W. S. (eds), Plenum Press, New York (1978)
8. Futai M. and Tanaka Y.; Localization of D-lactate dehydrogenase in membrane vesicles prepared by using a french press or ethylenediaminetetraacetate-lysozyme from Escherichia coli; *J. Bacteriol.* 124: 470-475 (1975)
9. Schmidt, T.G.M. and Skerra, A.; The Strep-tag system for one-step purification and high-affinity detection or capturing of proteins; *Nat. Protoc.* 2: 1528–1535 (2007)
10. Osyczka A., Moser C.C. and Dutton P.L.; Novel cyanide inhibition at cytochrome c<sub>1</sub> of Rhodobacter capsulatus cytochrome bc<sub>1</sub>, *BBA* 1655: 71-76 (2004)
11. Houchins J. P. and Hind G.; Concentration and Function of membrane-bound cytochromes in cyanobacterial heterocysts; *Plant Physiol.* 76: 456-460 (1984)
12. Valkova-Valchanova M.B., Saribas, A.S., Gibney B.R., Dutton P.L. and Daldal F.; Isolation and characterization of a two-subunit cytochrome bc<sub>1</sub> subcomplex from Rhodobacter capsulatus and reconstitution of its ubihydroquinone oxidation (Qo) site with purified Fe-S protein subunit; *Biochem.* 37: 16242-16251 (1998)

13. Sarewicz M., Borek A., Daldal F., Froncisz W. and Osyczka A.; Demonstration of short-lived complexes of cytochrome c with cytochrome bc<sub>1</sub> by EPR spectroscopy: implications for the mechanism of interprotein electron transfer; *J. Biol. Chem.* 283: 24826-24836 (2008)
14. Trumpower B.L. and Edwards C.A.; Purification of a reconstitutively active iron-sulphur protein (oxidation factor) from Succinate. Cytochrome c reductase complex of bovine heart mitochondria; *J. Biol. Chem.* 254: 8697-8706 (1979)
15. Cape, J.L., Strahan, J.R., Lenaeus, M.J., Yuknis, B.A., Le, T.T., Shepherd, J.N., Bowman, M.K., and Kramer, D.M.; The respiratory substrate rhodoquinol induces Q-cycle bypass reactions in the yeast cytochrome bc<sub>1</sub> complex - mechanistic and physiological implications; *J. Biol. Chem.* 280: 34654–34660. (2005)
16. Muller, F., Crofts, A.R., and Kramer, D.M.; Multiple Q-cycle bypass reactions at the Q<sub>o</sub> site of the cytochrome bc<sub>1</sub> complex; *Biochem.* 41: 7866-7874 (2002)
17. Kramer D.M., Roberts A.G., Muller F., Cape J. and Bowman M.K.; Q-cycle bypass reactions at the Q<sub>o</sub> site of the cytochrome bc<sub>1</sub> (and related) complexes; *Methods. Enzymol.* 382: 21-45 (2004)
18. Brandt U., Yu L., Yu C. and Trumpower B.L.; The mitochondrial targeting presequence of the rieske iron-sulfur protein is processed in a single step after Insertion into the Cytochrome bc<sub>1</sub> Complex in Mammals and Retained as a Subunit in the Complex, *J. Biol. Chem.* 268(12): 8387-8390 (1993)
19. Robertson D.E., Davidson E., Prince R.C., van den Berg W.H., Marrsll B.L. and Dutton P.L.; Discrete catalytic sites for quinone in the ubiquinol-cytochrome c<sub>2</sub> oxidoreductase of *Rhodospseudomonas capsulata* – evidence from a mutant defective in ubiquinol oxidation; *J. Biol. Chem.* 261(2): 584-591 (1986)
20. Hagen W.R.; The Spectrometer. In: Biomolecular EPR spectroscopy 9-32; CRC Press, New York (2009)
21. Czaplá M., Borek A., Sarewicz M. and Osyczka A.; Enzymatic activities of isolated cytochrome bc<sub>1</sub>-like complexes containing fused cytochrome b subunits with asymmetrically inactivated segments of electron transfer chains; *Biochem.* 51(4): 829–835 (2012)
22. Zhang H., Chobot S.E., Osyczka A., Wraight C.A., Dutton P.L. and Moser C.C; Quinone and non-quinone redox couples in Complex III; *J Bioenerg Biomembr.* 40: 493-499 (2008)
23. Sarewicz M., Dutka M., Pintscher S. and Osyczka A.; Triplet state of the semiquinone-rieske cluster as an intermediate of electronic bifurcation catalyzed by cytochrome bc<sub>1</sub>; *Biochem.* 52: 6388-6395 (2013)
24. Grey K.A., Dutton L.P. and Daldal F.; Requirement of histidine 217 for ubiquinone reductase activity (Q<sub>i</sub> site) in the cytochrome bc<sub>1</sub> complex; *Biochem.* 33: 723-733 (1994)